

Biologically guided isolation and ADMET profile of new Factor Xa inhibitors from *Glycyrrhiza glabra* roots using *in-vitro* and *in-silico* approaches

Reham S. Ibrahim, ^{*a}, Rahma SR. Mahrous, ^a Rasha M. Abu EL-Khair, ^a
Samir A. Ross, ^{b,c} Abdallah A. Omar ^a and Hoda M. Fathy ^a

^aDepartment of Pharmacognosy, Faculty of Pharmacy, Alexandria, Egypt;

^bNational Center for Natural Products Research, University of Mississippi, Thad Cochran Research Center, Oxford, MS, USA;

^cBioMolecular Sciences, Division of Pharmacognosy, School of Pharmacy, University of Mississippi, University, MS, USA

*Corresponding author. E-mail: rehamsaid84@yahoo.com,

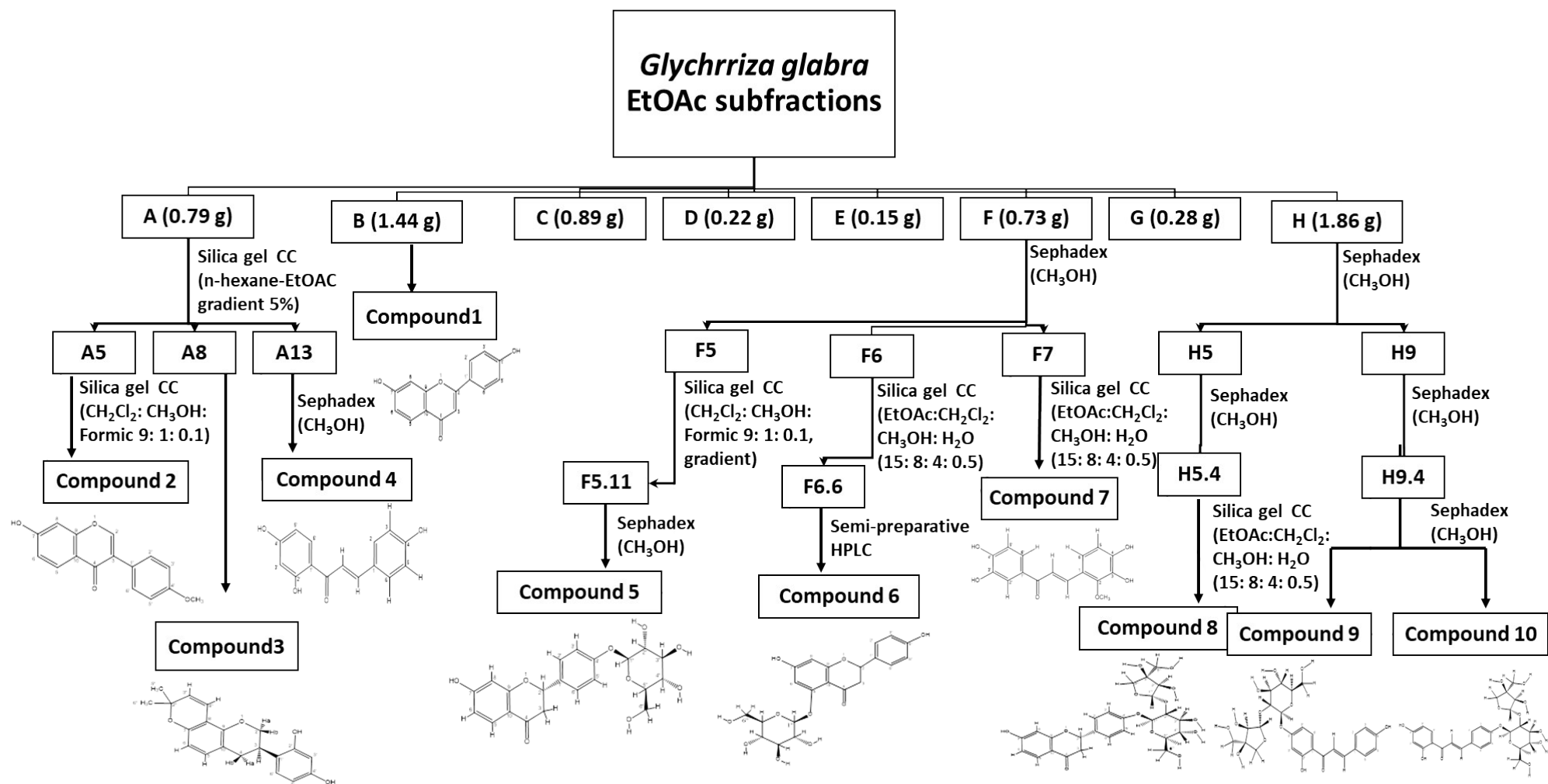


Fig. S1 Scheme for the isolation of 10 compounds from EtOAc subfractions of the roots of *G. glabra*

Table S1. % inhibition of different fractions of *G. glabra* roots extract on FXa*

Fraction	Concentration (mg/ml)	% Inhibition (%)
Light petroleum	1.5	1.55±0.056
	3	0.69±0.083
CH ₂ Cl ₂	1.5	62.31±0.097
	3	71.94±0.034
EtOAc	1.5	87.26±0.034
	3	97.93±0.019
n-BuOH	1.5	13.08±0.095
	3	21.51±0.04
Rivaroxaban (positive control)	100 nM	88.64±0.76

* Inhibition rate was expressed as mean±SD, n=2

Table S2. *In-vitro* % inhibition of EtOAc subfractions of *G. glabra* on FXa enzyme

Subfraction# (1 mg/ml)	% inhibition
(A)	60.94±1.18
(B)	61.03±1.99
(C)	63.85±0.18
(D)	65.64±0.45
(E)	77.66±0.66
(F)	84.94±0.82
(G)	76±0.87
(H)	77.39±0.46

Subfractions are arranged according to polarities from the least polar; A to the most polar; H

* Inhibition rate was expressed as mean±SD, n=2

Table S3. continued

δH (J in Hz)											
Position	(1)	(2)	(3)	(5)	(6)	(8)	Position	(4)	(7)	(9)	(10)
- β -Glu moiety						- β -Glu moiety					
1"	-	-	-	4.94, d (7.94)	4.75, d (7.2)	5.00, d (7.47)	1"	-	-	5.09, d (6.1)	5.05, d (7.33)
2"	-	-	-	3.43- 3.47, m	3.53, m	3.66, m	2"	-	-	3.67, m	3.67, m
3"	-	-	-	3.43- 3.47, m	3.44, m	3.66, m	3"	-	-	3.49, m	3.49, m
4"	-	-	-	3.43- 3.47, m	3.65, s	3.40- 3.44, m	4"	-	-	3.43, m	3.42, m
5"	-	-	-	3.43- 3.47, m	3.49	3.40- 3.44, m	5"	-	-	3.98, d (1.58)	3.97, d (1.62)
6"	-	-	-	Ha: 3.70, dd (12.05, 5.44) Hb: 3.90, d (11.90, 2.07)	Ha: 3.67, t (12) Hb: 3.92, t (11)	Ha: 3.70, m (12.13) Hb: 3.89, dd (12.17, 2.17)	6"	-	-	Ha: 3.73, m Hb: 3.91, d (12.23)	Ha: 3.71, m Hb: 3.91, d (12.18)
- β -Api moiety						- β -Api moiety					
1'''	-	-	-	-	-	5.48, d (1.47)	1'''	-	-	5.48, dd (5.23, 1.62)	5.47, dd (5.66, 1.62)
2'''	-	-	-	-	-	3.96, d (1.52)	2'''	-	-	3.67, m	3.67, m
3'''	-	-	-	-	-	-	3'''	-	-	-	-
4'''	-	-	-	-	-	Ha: 3.80, d (9.53) Hb: 4.06, d (9.60)	4'''	-	-	Ha: 3.82, d (9.56) Hb: 4.05, t (10.15)	Ha: 3.81, d (9.59) Hb: 4.05, dd (11.76, 9.61)
5'''	-	-	-	-	-	3.55, d (2.50)	5'''	-	-	3.55, d (2.17)	3.55, d (2.17)

Table S4. ¹³C-NMR spectral data of compounds (1- 10), δ values in ppm

δ C (ppm)											
Position	(1)	(2)	(3)	(5)	(6)	(8)	Position	(4)	(7)	(9)	(10)
2	162.70	153.45	69.98	80.85	79.98	80.89	C- α	118.54	120.77	117.94	120.17
3	104.49	124.86	31.46	45.11	46.47	45.06	C- β	145.72	141.09	146.52	144.94
4	176.39	175.77	30.38	193.35	192.59	193.36	C=O	193.74	191.65	194.02	193.48
5	126.50	128.53	129.09	130.01	162.94	130.02	1	128.01	121.63	127.82	130.61
6	114.89	115.75	108.78	112.04	102.06	112.00	2, 6	131.96	150.07	132.15	131.57
7	162.53	163.34	151.53	167.11	164.97	166.99	3, 5	117.10	139.84	117.09	117.93
8	102.51	103.21	109.94	104.01	100.96	103.99	4	161.68	150.90	161.81	161.02
9	157.44	158.77	149.58	165.55	166.84	165.53	5	117.10	112.90	117.09	117.93
10	116.09	118.59	114.65	115.08	103.90	115.10	6	131.96	120.55	132.15	131.57
1'	121.82	125.63	120.04	134.58	131.58	134.48	1'	114.71	131.98	116.67	114.81
2'	128.16	131.08	154.51	128.92	129.06	128.98	2'	166.48	116.53	166.92	165.00
3'	115.96	114.48	103.16	117.94	116.42	117.74	3'	104.06	146.72	105.03	103.98
4'	160.74	160.41	154.88	159.36	159.01	159.21	4'	166.48	152.27	164.96	167.69
5'	115.96	114.48	107.83	117.94	116.42	117.74	5'	109.55	116.10	110.95	109.38
6'	128.16	131.08	128.29	128.92	129.06	128.98	6'	133.51	123.57	133.14	133.61
OCH3-4'	-	55.63	-	-	-	-	OCH3-2	-	61.90	-	-
2''	-	-	75.86	-	-	-	-	-	-	-	-
3''	-	-	129.24	-	-	-	-	-	-	-	-
4''	-	-	116.83	-	-	-	-	-	-	-	-
5''	-	-	27.61	-	-	-	-	-	-	-	-
6''	-	-	27.41	-	-	-	-	-	-	-	-
- β -Glu moiety							- β -Glu moiety				
1'''	-	-	-	102.32	105.45	100.92	1'''	-	-	100.03	100.51
2'''	-	-	-	75.04	74.90	78.73	2'''	-	-	78.63	78.79
3'''	-	-	-	78.11	77.36	78.75	3'''	-	-	78.25	78.30
4'''	-	-	-	71.50	71.34	71.52	4'''	-	-	71.31	71.51
5'''	-	-	-	78.31	78.74	78.23	5'''	-	-	78.74	78.71
6'''	-	-	-	62.64	62.61	62.61	6'''	-	-	62.47	62.64
- β -Api moiety							- β -Api moiety				
1''''	-	-	-	-	-	110.92	1''''	-	-	109.45	110.93
2''''	-	-	-	-	-	78.16	2''''	-	-	78.65	78.79
3''''	-	-	-	-	-	80.82	3''''	-	-	80.89	80.88
4''''	-	-	-	-	-	75.60	4''''	-	-	75.59	75.69
5''''	-	-	-	-	-	66.18	5''''	-	-	66.11	66.19

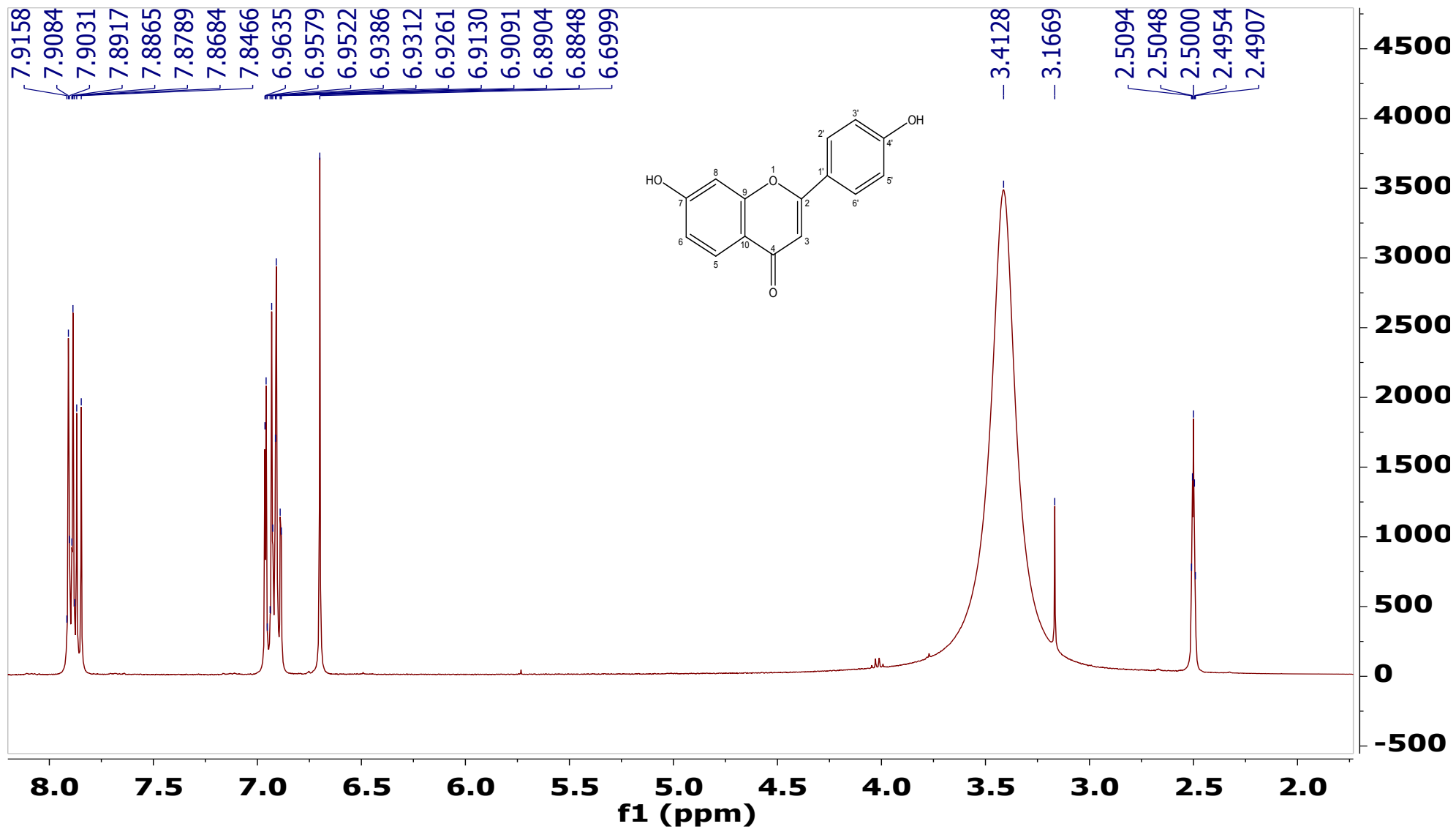


Fig. S2 ¹H-NMR spectrum of 7, 4'-dihydroxyflavone (1) in DMSO, d₆ at 400 MHz

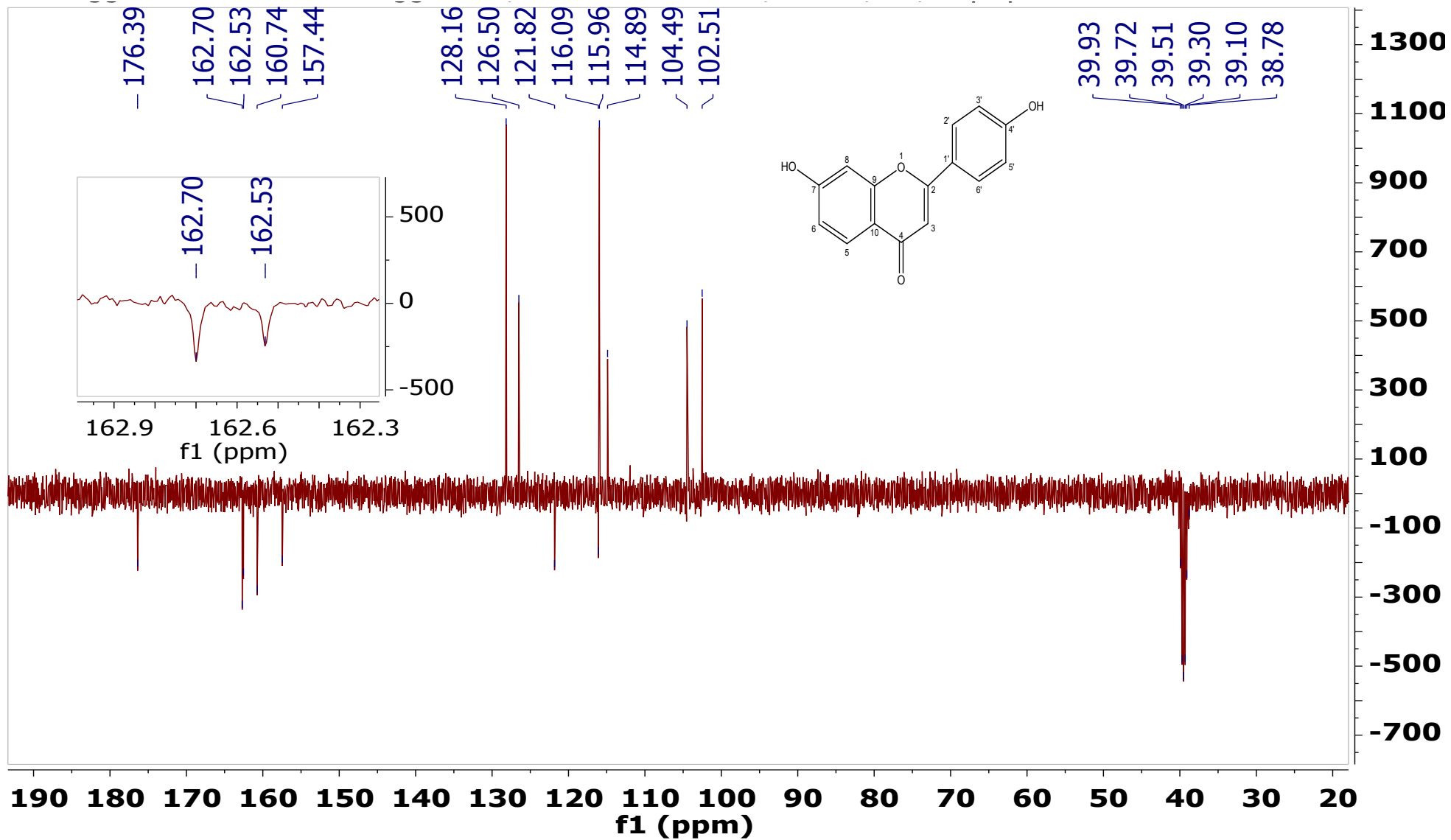


Fig. S3 ^{13}C -DEPTQ spectrum of 7, 4'-dihydroxyflavone (1) in DMSO, d6 at 100 MHz (with expansion at 162.3-162.9 ppm)

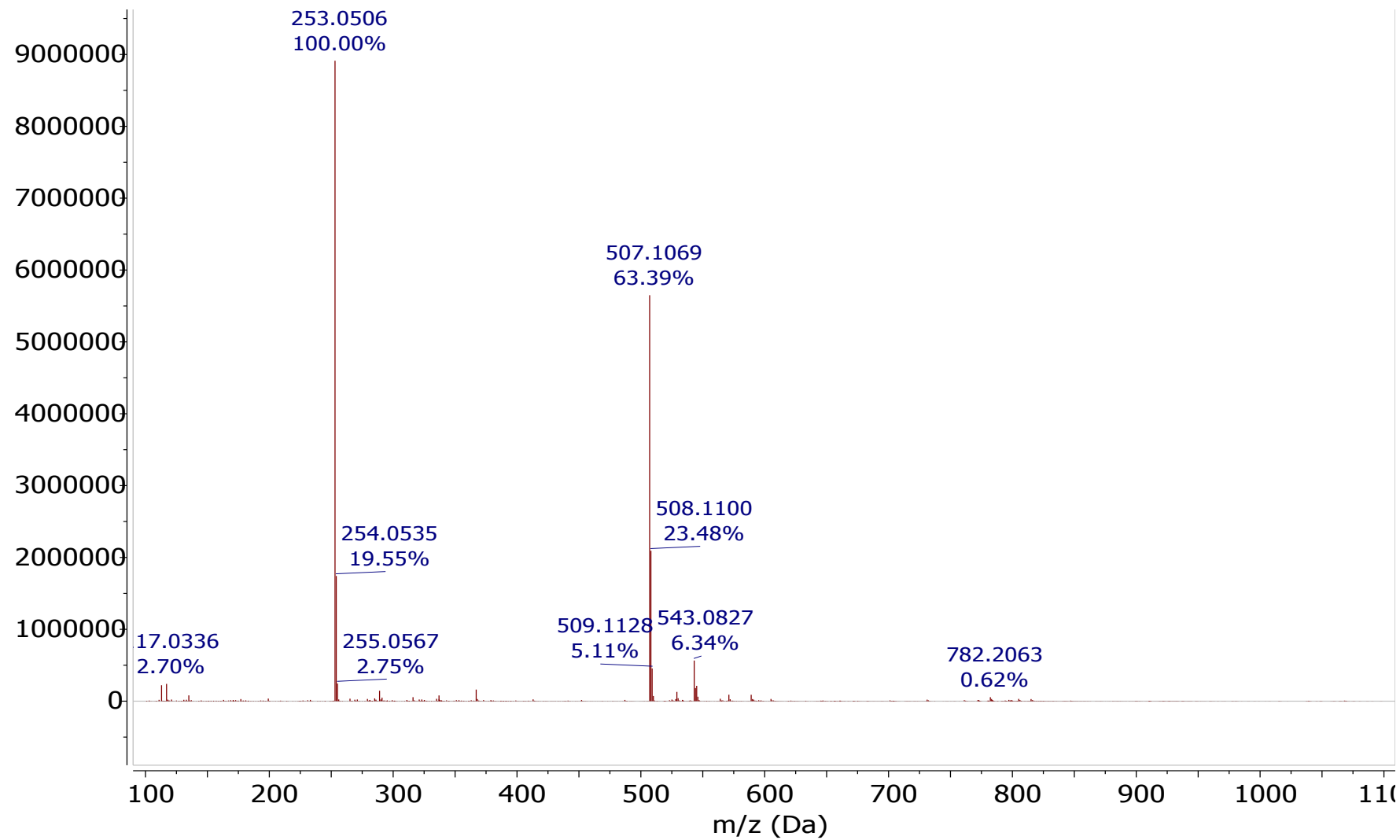


Fig. S4 HRESIMS spectrum of 7, 4'-dihydroxyflavone (1) in negative mode

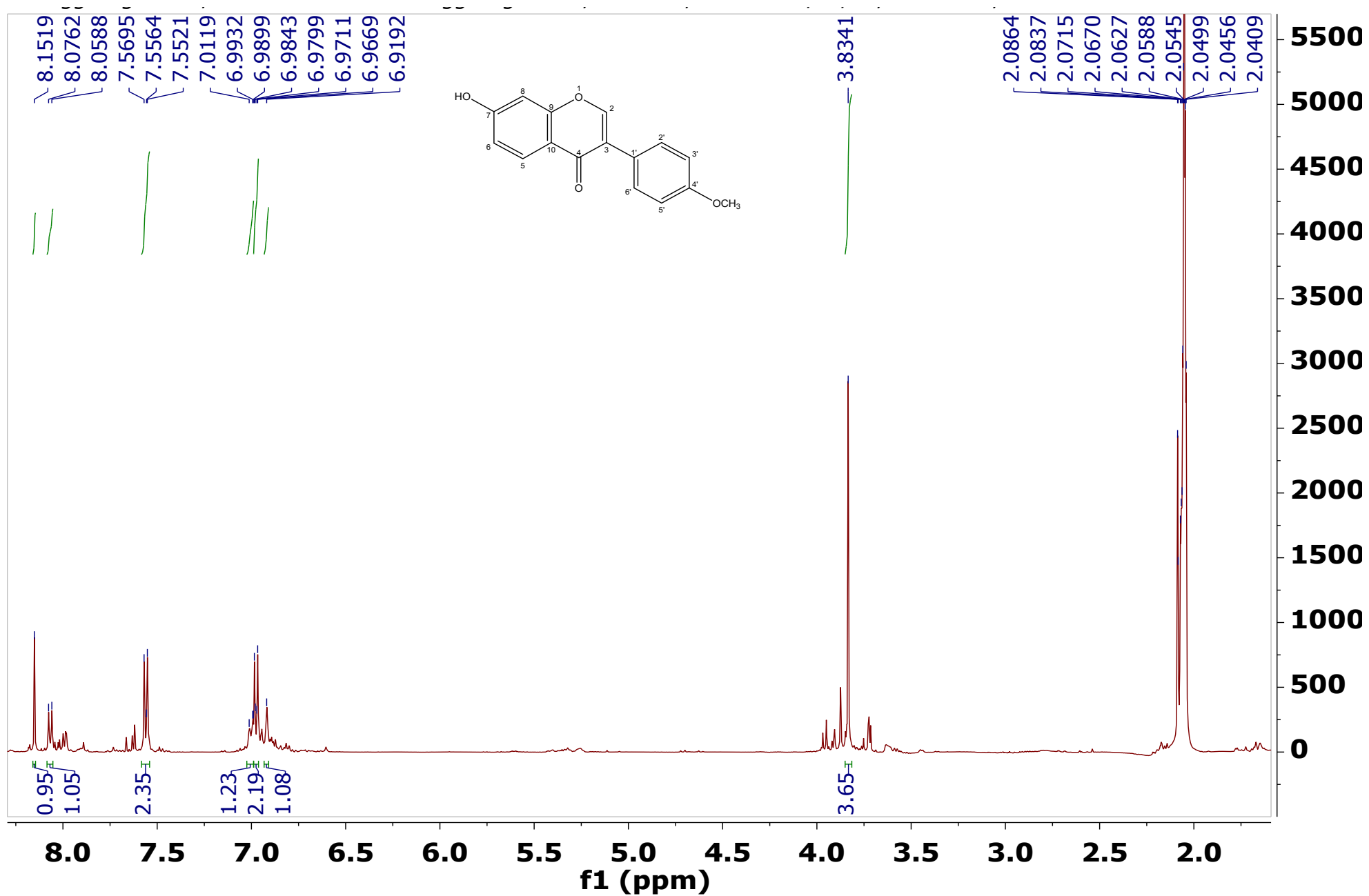


Fig. S5 ¹H-NMR spectrum of 7-hydroxy-4'-methoxyisoflavone (2) in Acetone, d₆ at 500 MHz

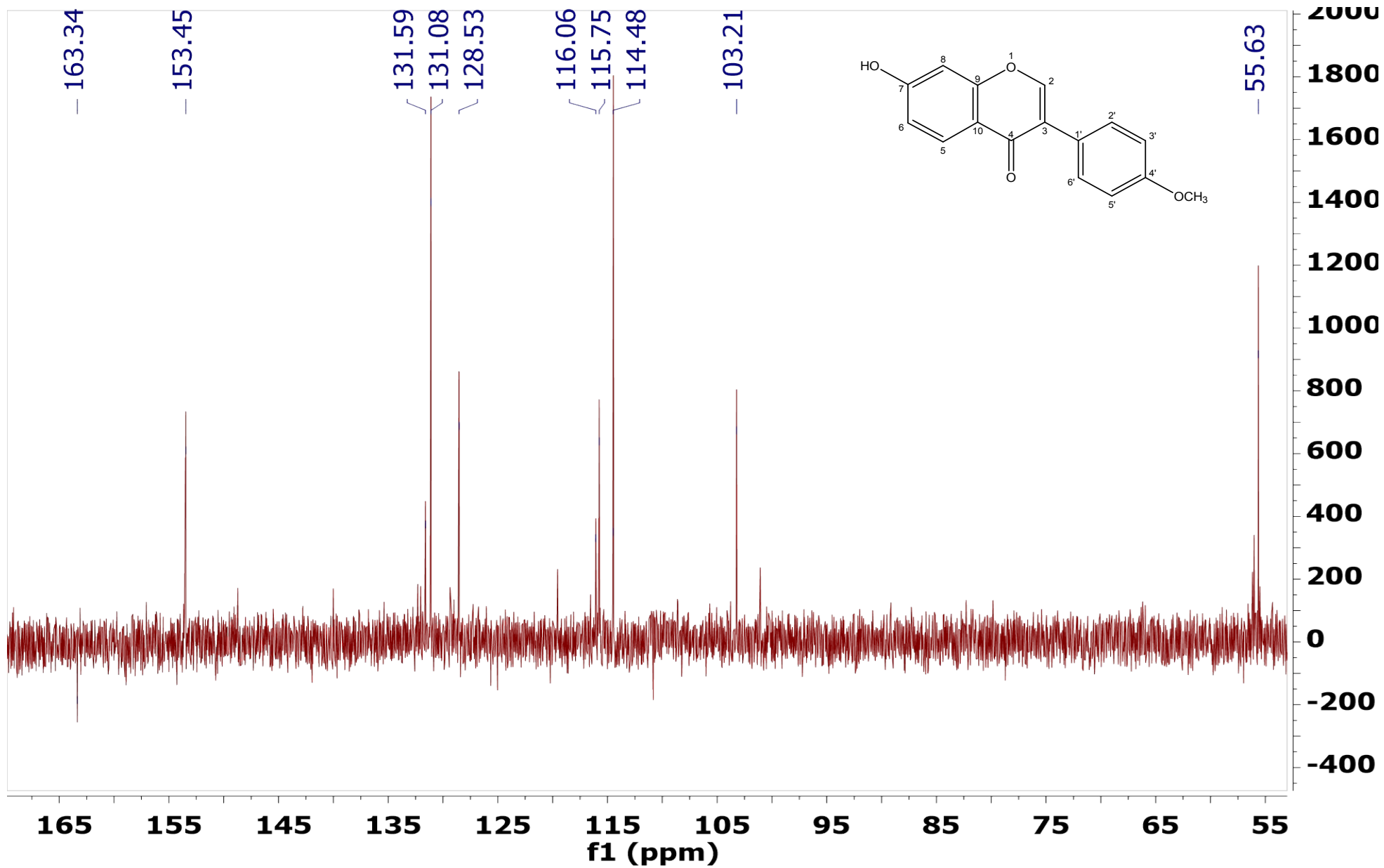


Fig. S6 ^{13}C -DEPTQ spectrum of 7-hydroxy-4'-methoxyisoflavone (2) in Acetone, d_6 at 100 MHz

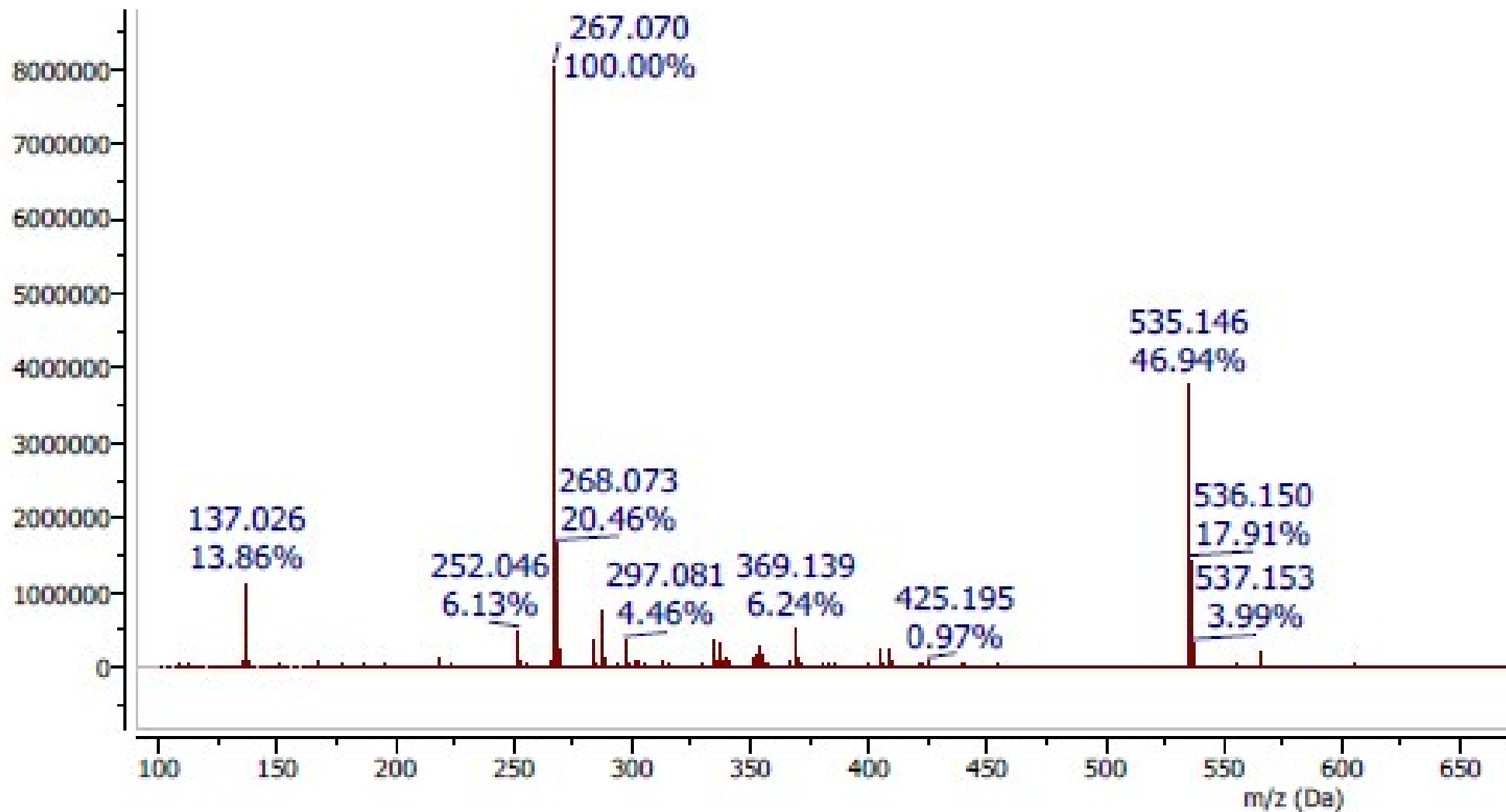


Fig. S7 HRESIMS spectrum of 7-hydroxy-4'-methoxyisoflavone (2) in negative mode

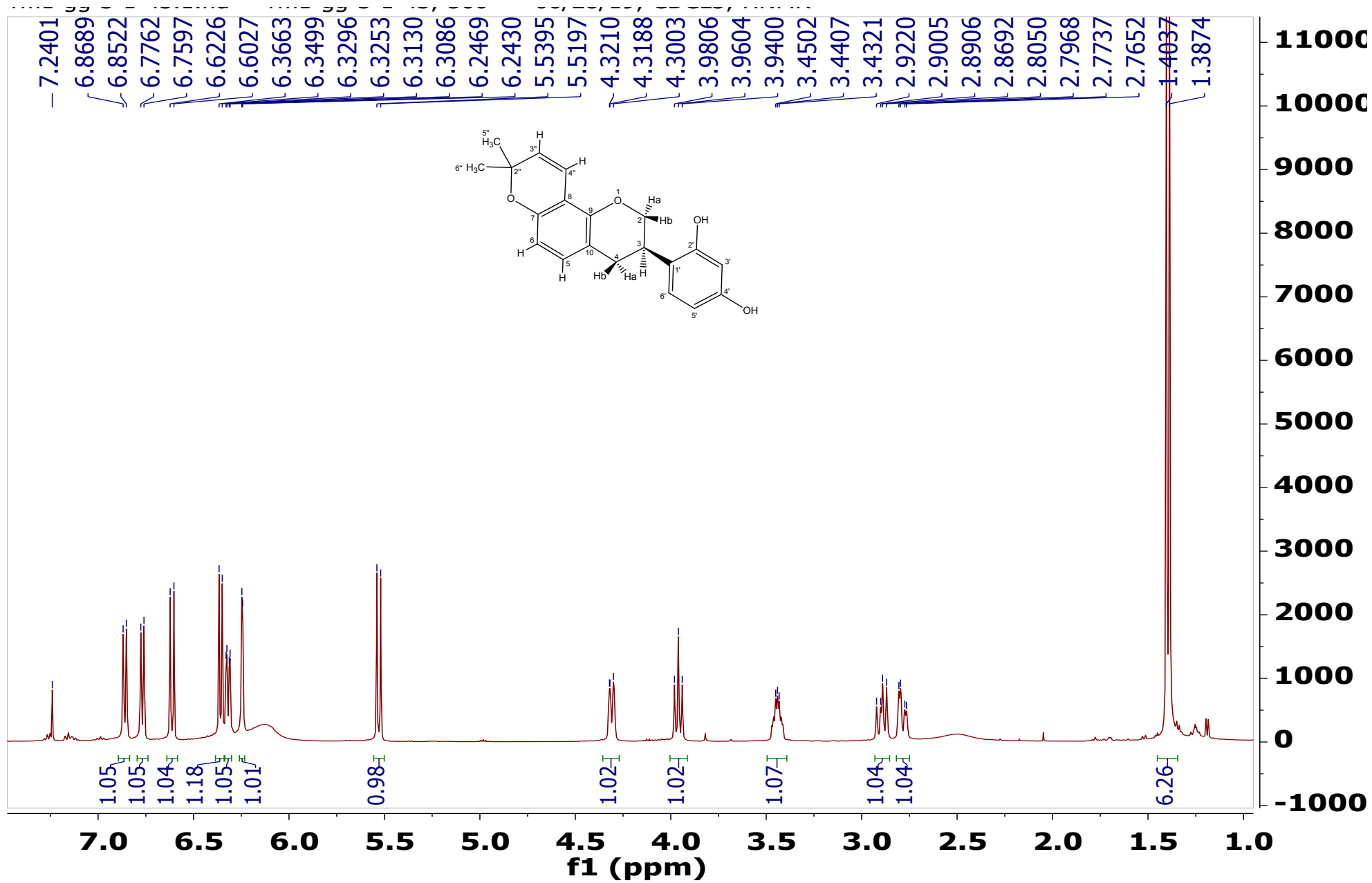


Fig. S8 $^1\text{H-NMR}$ spectrum of 3-R-glabridin (3) in CDCl_3 at 500 MHz

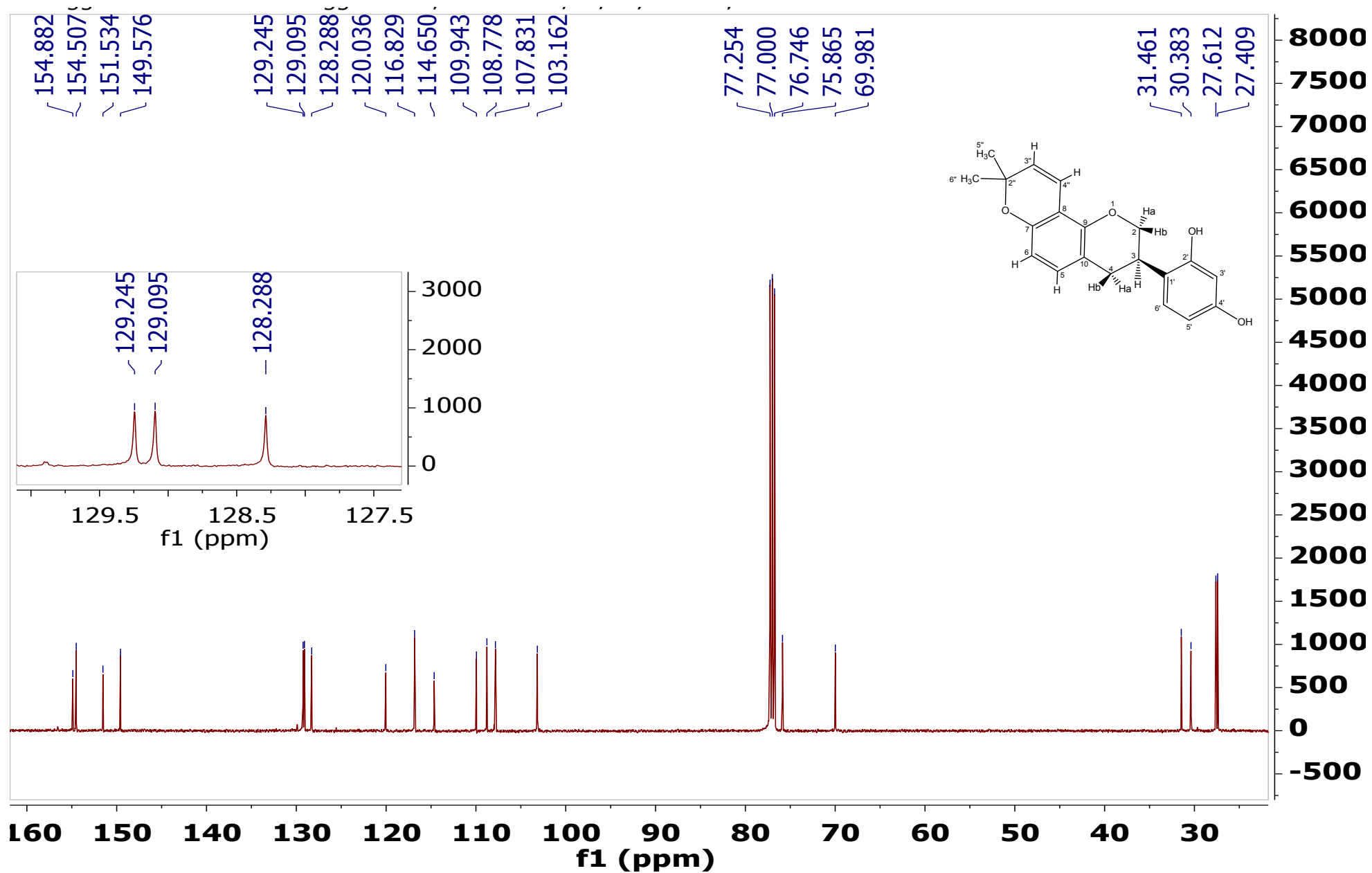


Fig. S9 ¹³C-NMR spectrum of 3-R-glabridin (3) in CDCl₃ at 125 MHz with expansion at (127.5- 129.5 ppm)

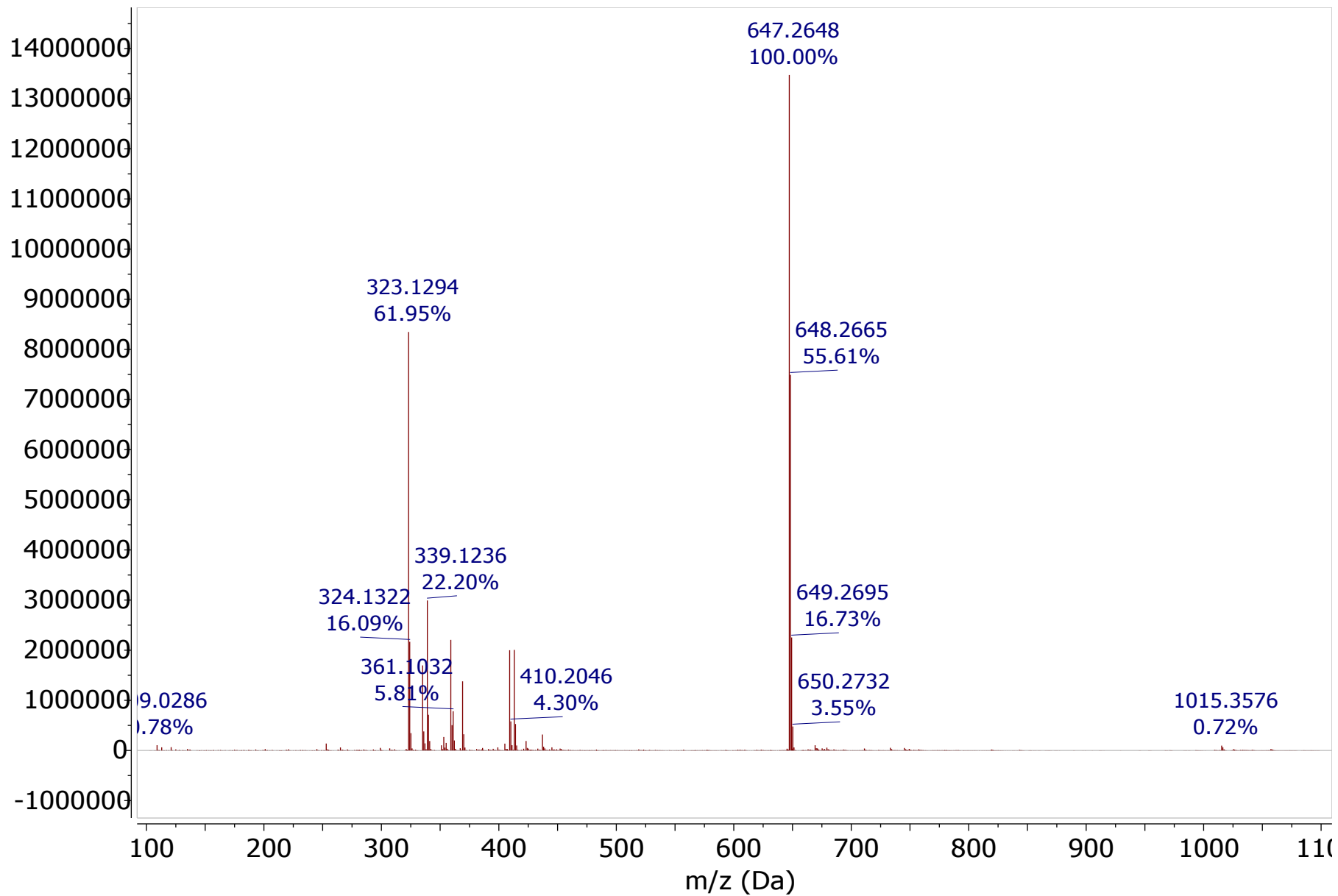


Fig. S10 HRESIMS spectrum of 3-R-glabridin (3) in negative mode

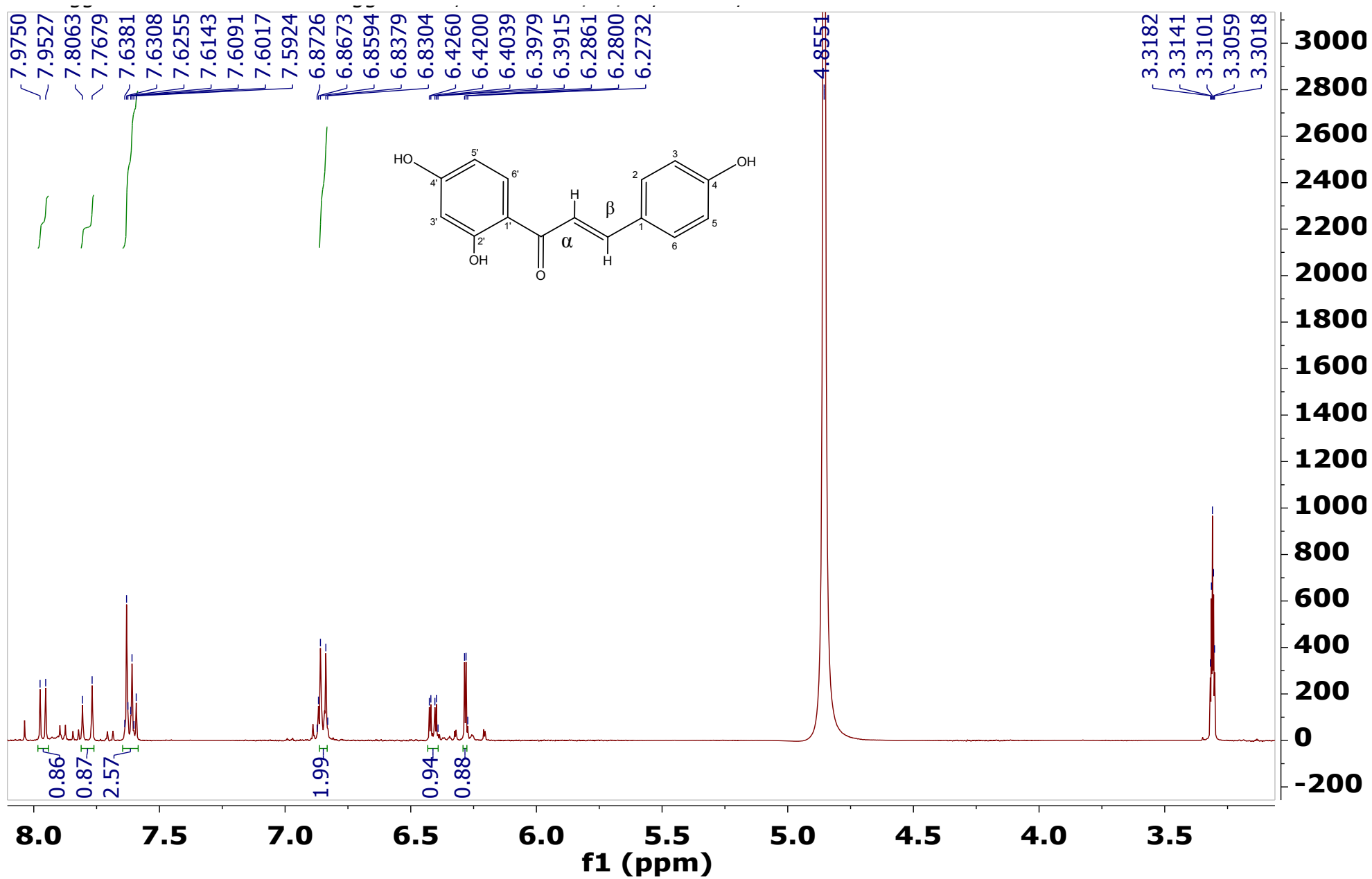


Fig. S11 $^1\text{H-NMR}$ spectrum of isoliquirtigenin (4) in CD_3OD at 400 MHz

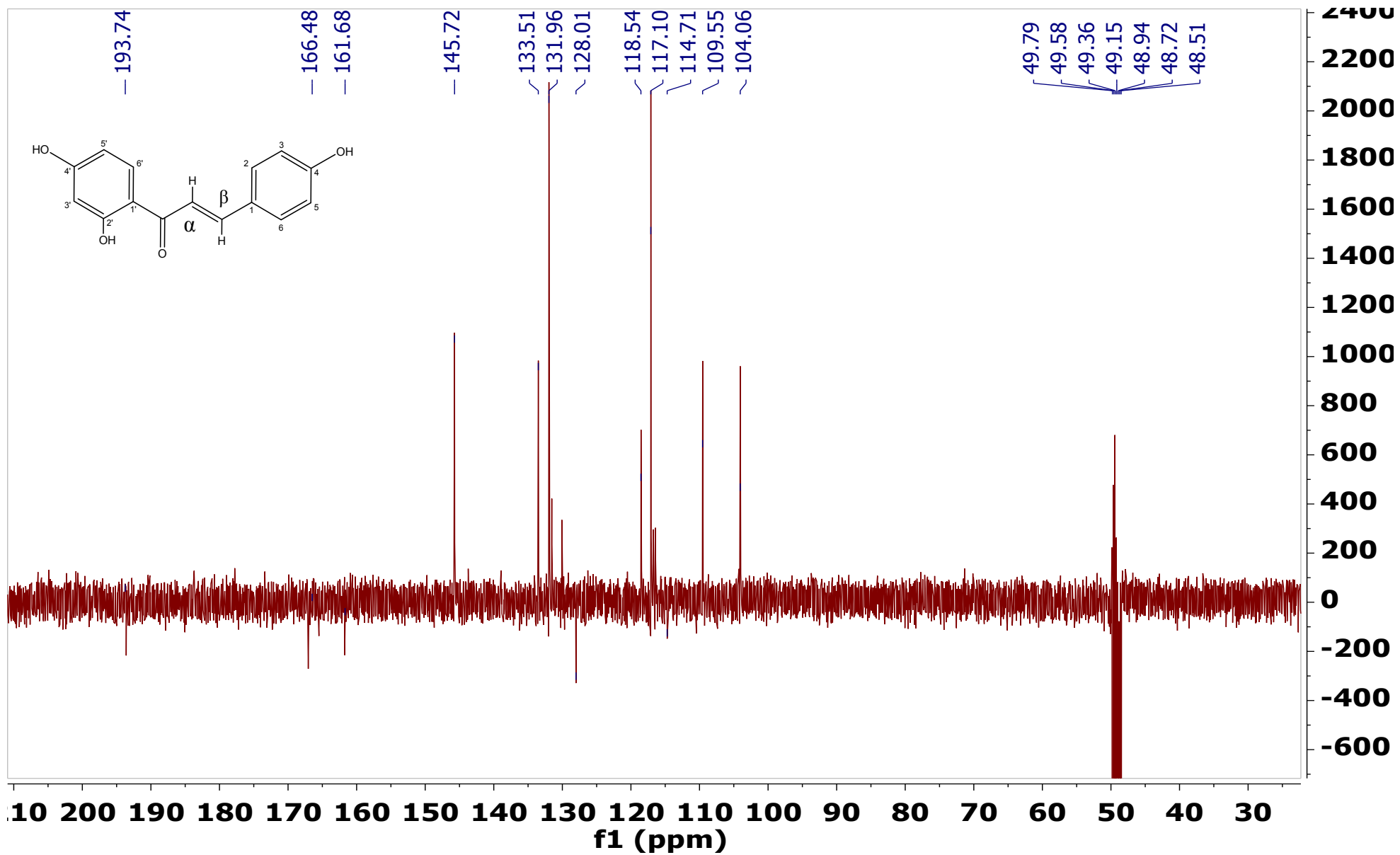


Fig. S12 ^{13}C -DEPTQ spectrum of isoliquirtigenin (4) in CD_3OD at 100 MHz

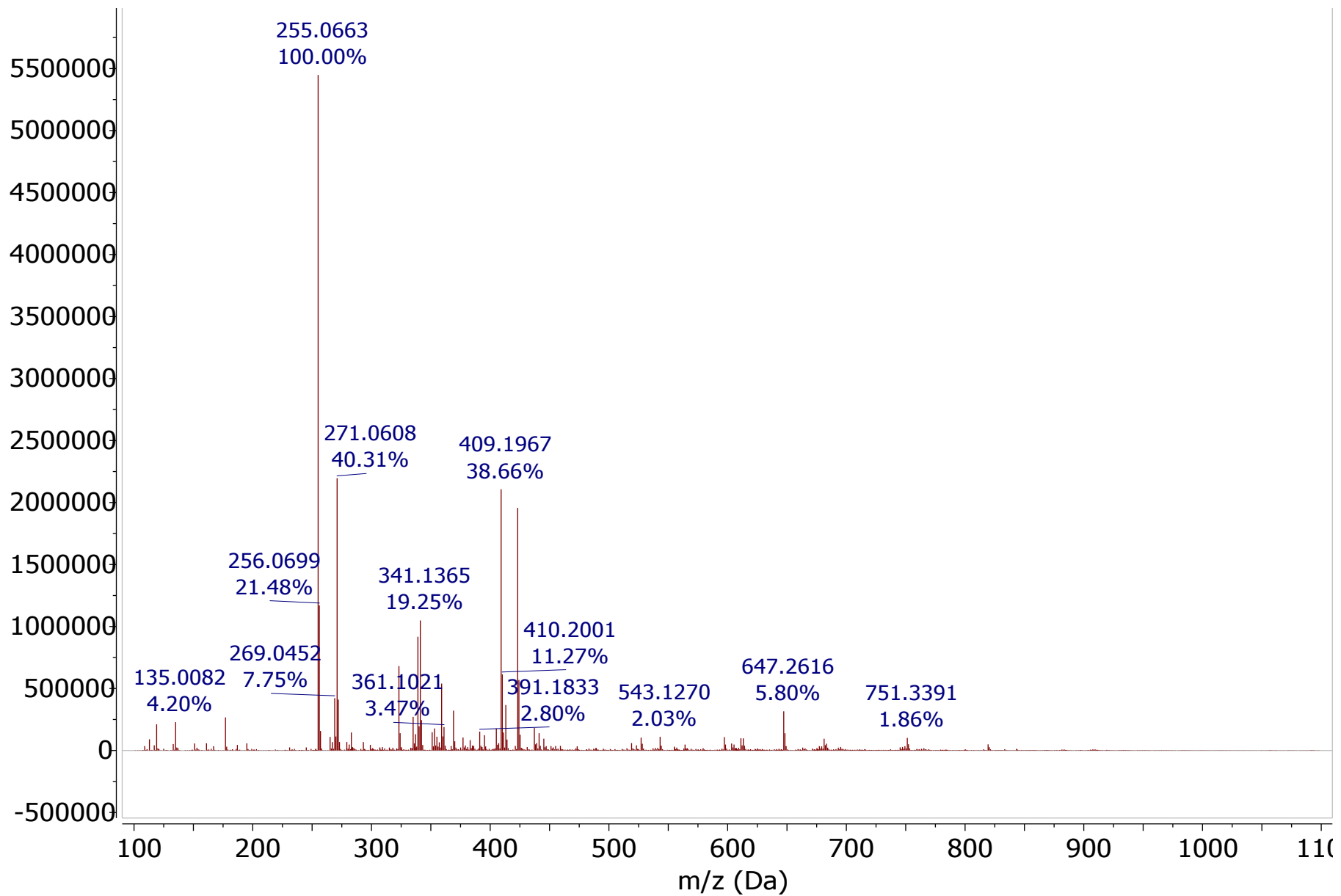


Fig. S13 HRESIMS spectrum of isoliquirtigenin (4) in negative mode

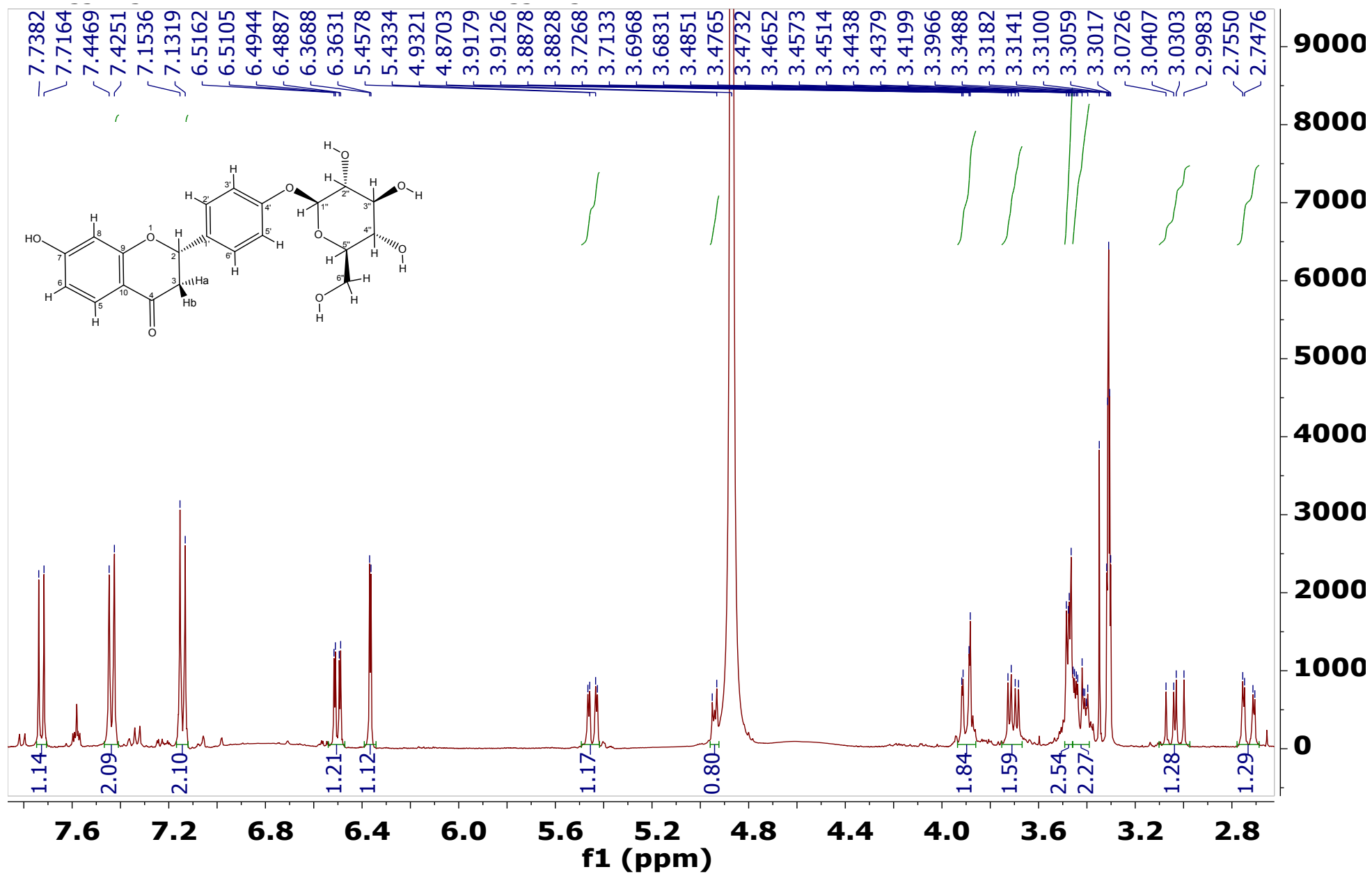


Fig. S14 ¹H-NMR spectrum of liquirtin (5) in CD₃OD at 400 MHz

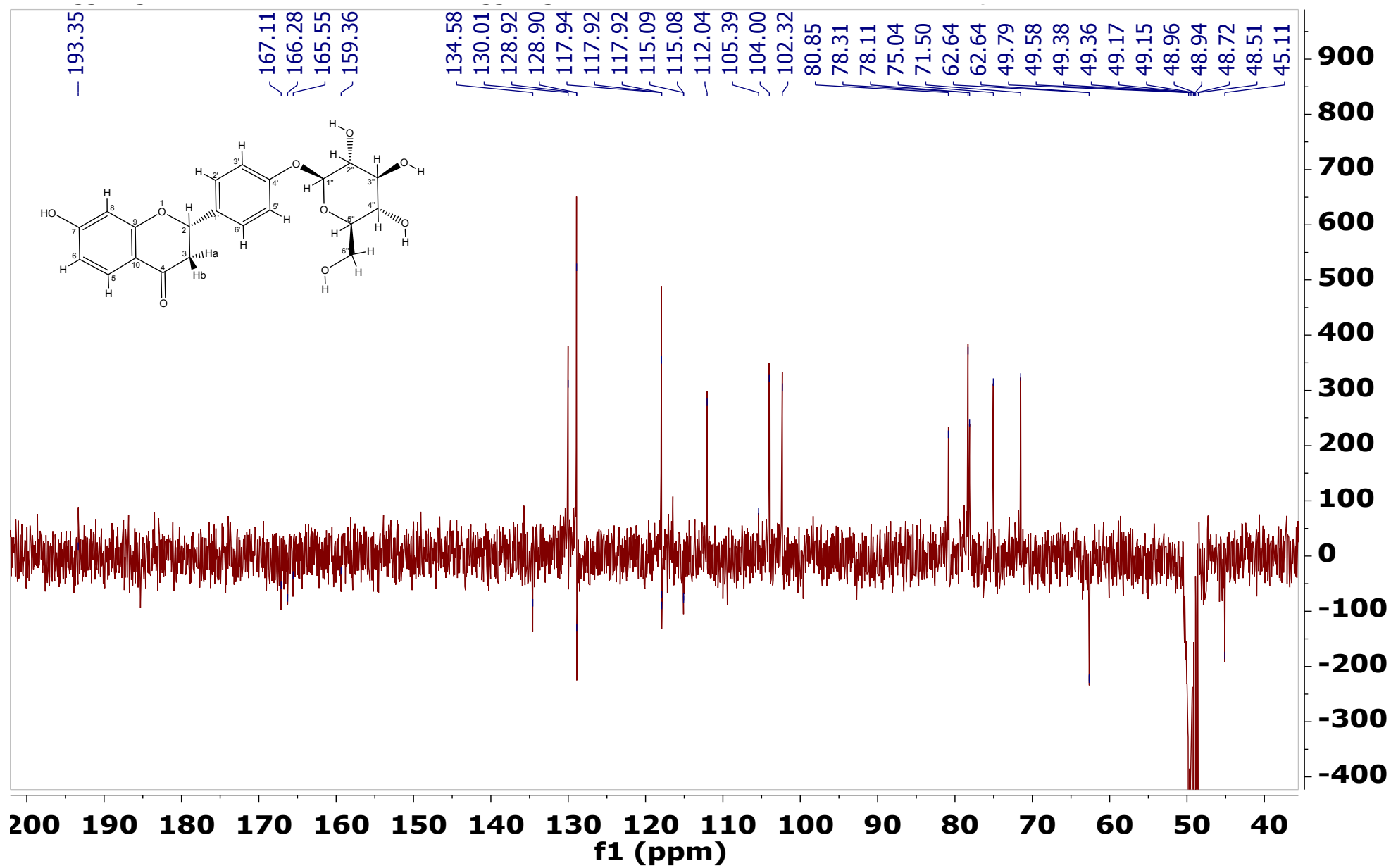


Fig. S15 ^{13}C -DEPTQ spectrum of liquiritin (5) in CD_3OD at 100 MHz

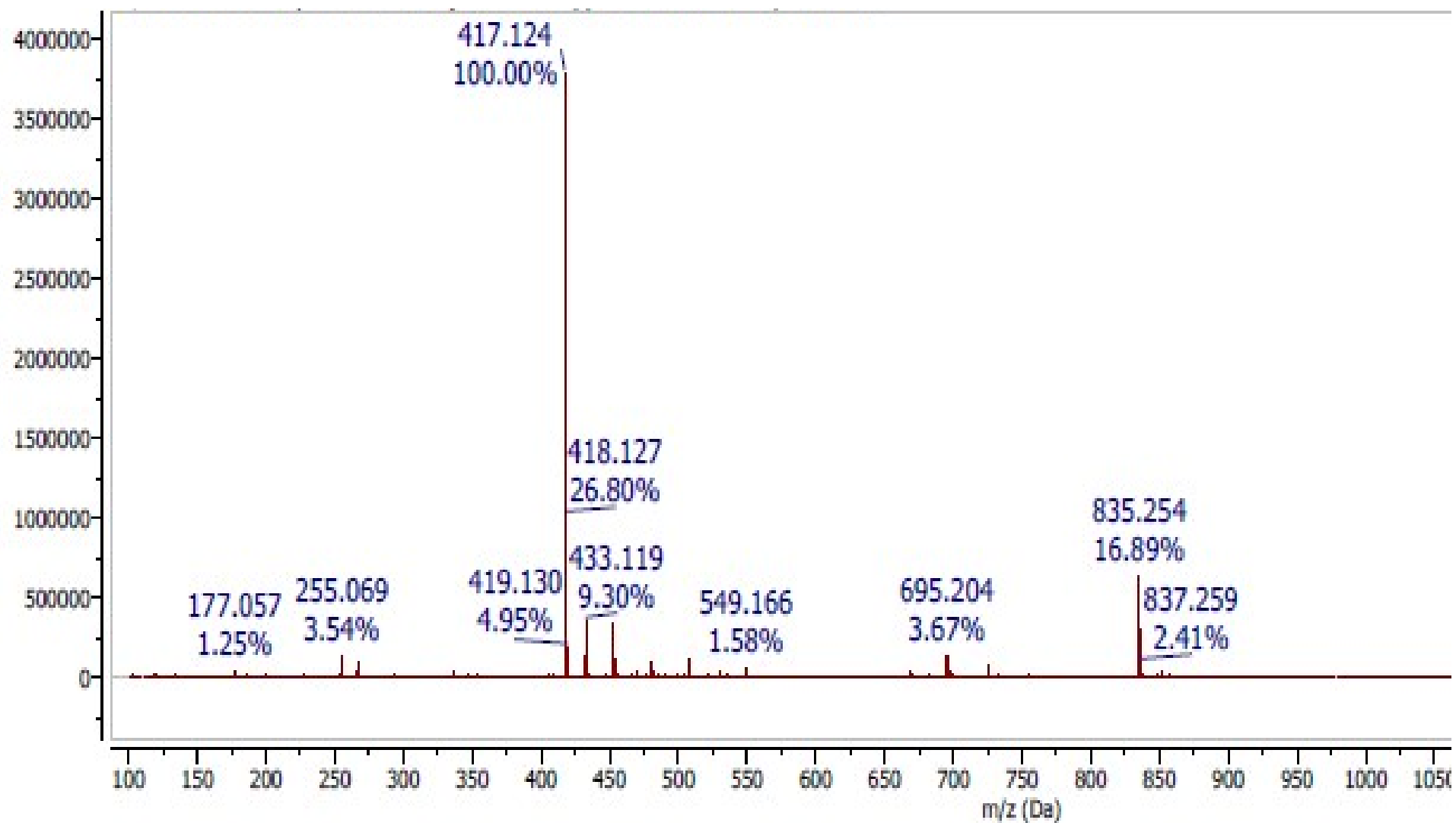


Fig. S16 HRESIMS spectrum of liquirtin (5) in negative mode

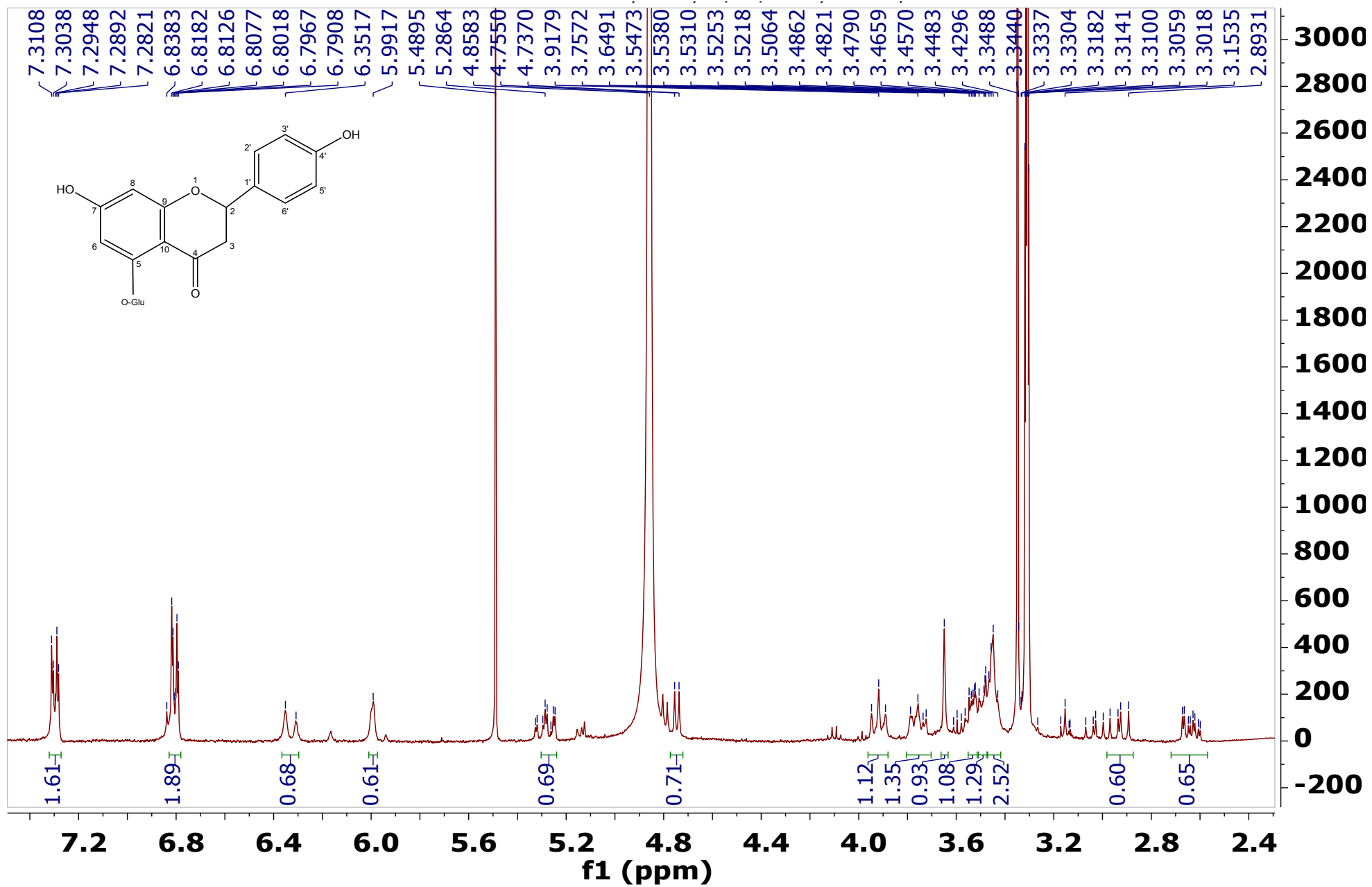


Fig. S17 ¹H-NMR spectrum of naringenin 5-O-glucoside (6) in CD₃OD at 400 MHz

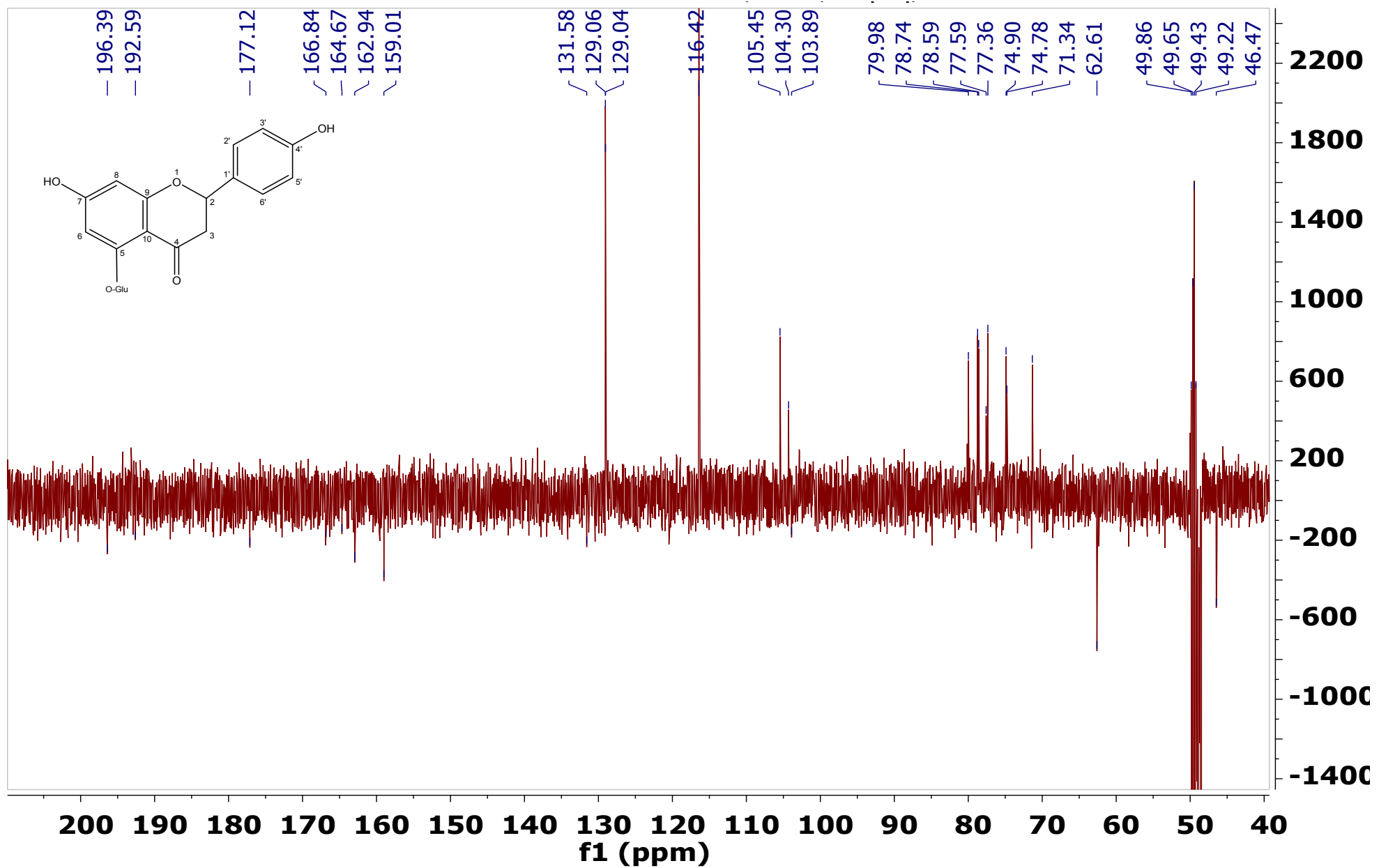


Fig. S18 ^{13}C -DEPTQ spectrum of naringenin 5-O-glucoside (6) in CD_3OD at 100 MHz

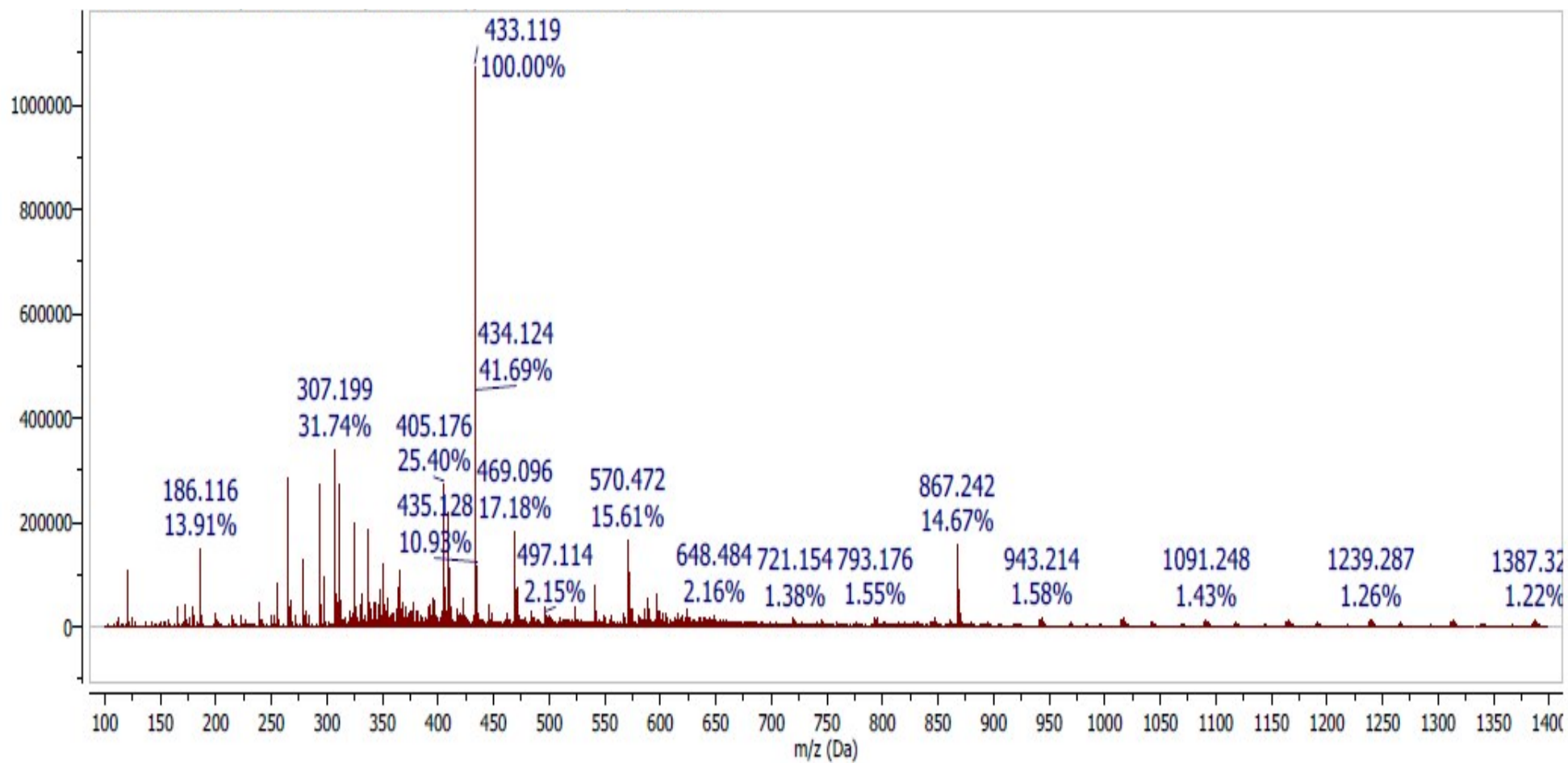


Fig. S19 HRESIMS spectrum of naringenin 5-O-glucoside (6) in negative mode

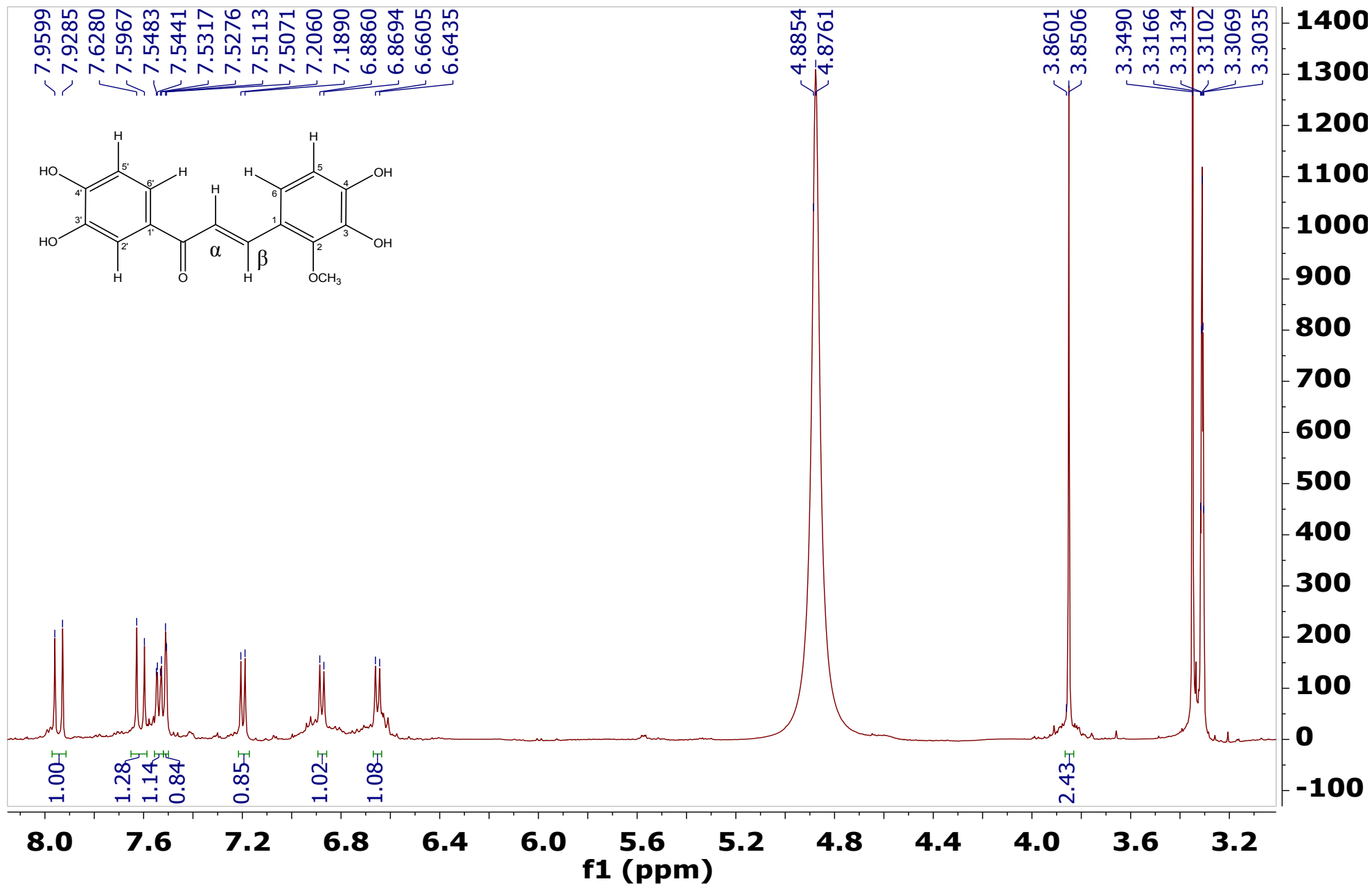


Fig. S20 $^1\text{H-NMR}$ spectrum of 3,3',4,4'-tetrahydroxy-2-methoxychalcone (7) in CD_3OD at 400 MHz

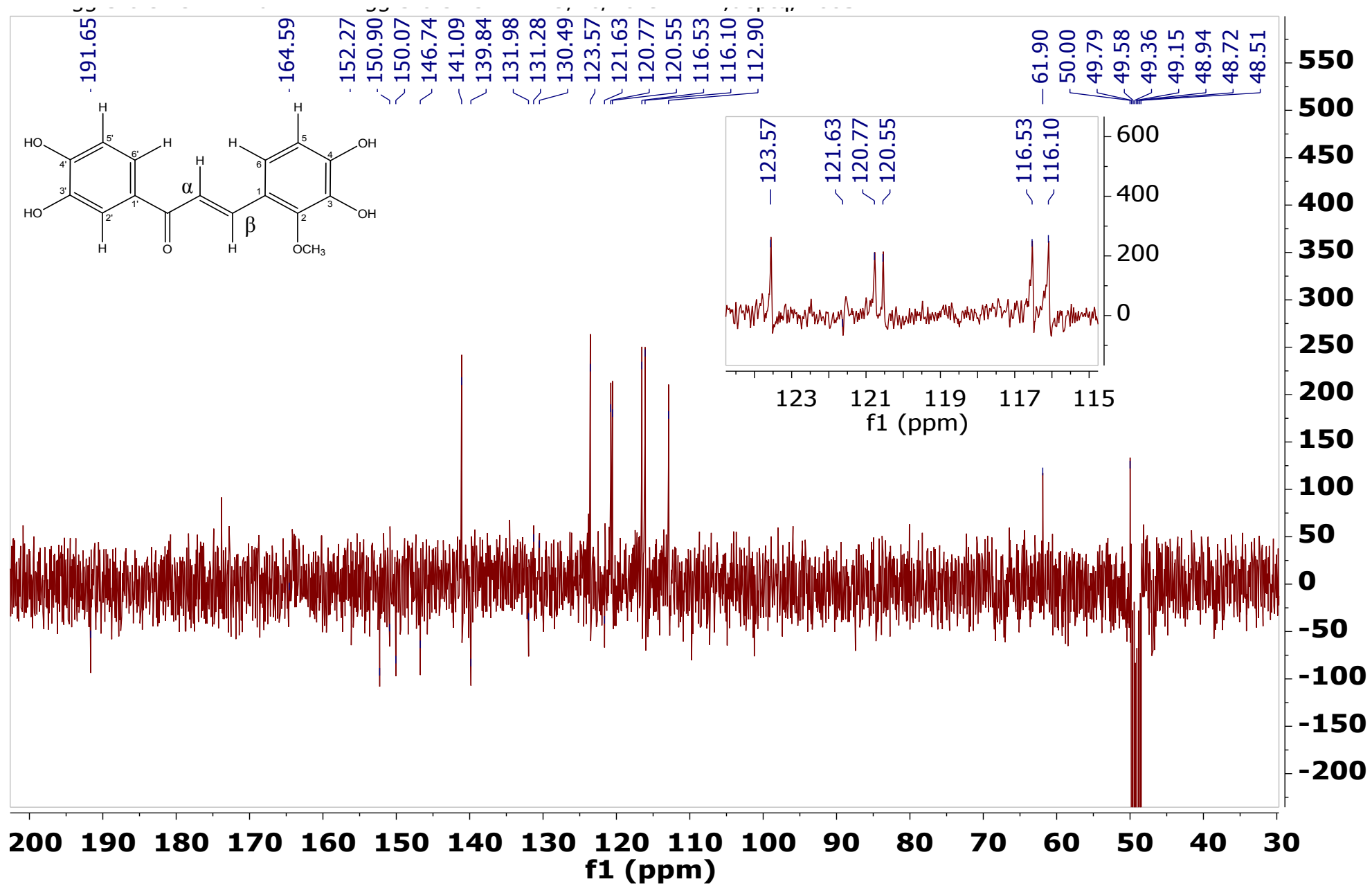


Fig. S21 ¹³C-DEPTQ spectrum of 3,3',4,4'-tetrahydroxy-2-methoxychalcone (7) in CD₃OD at 100 MHz with expansion at (115- 123 ppm)

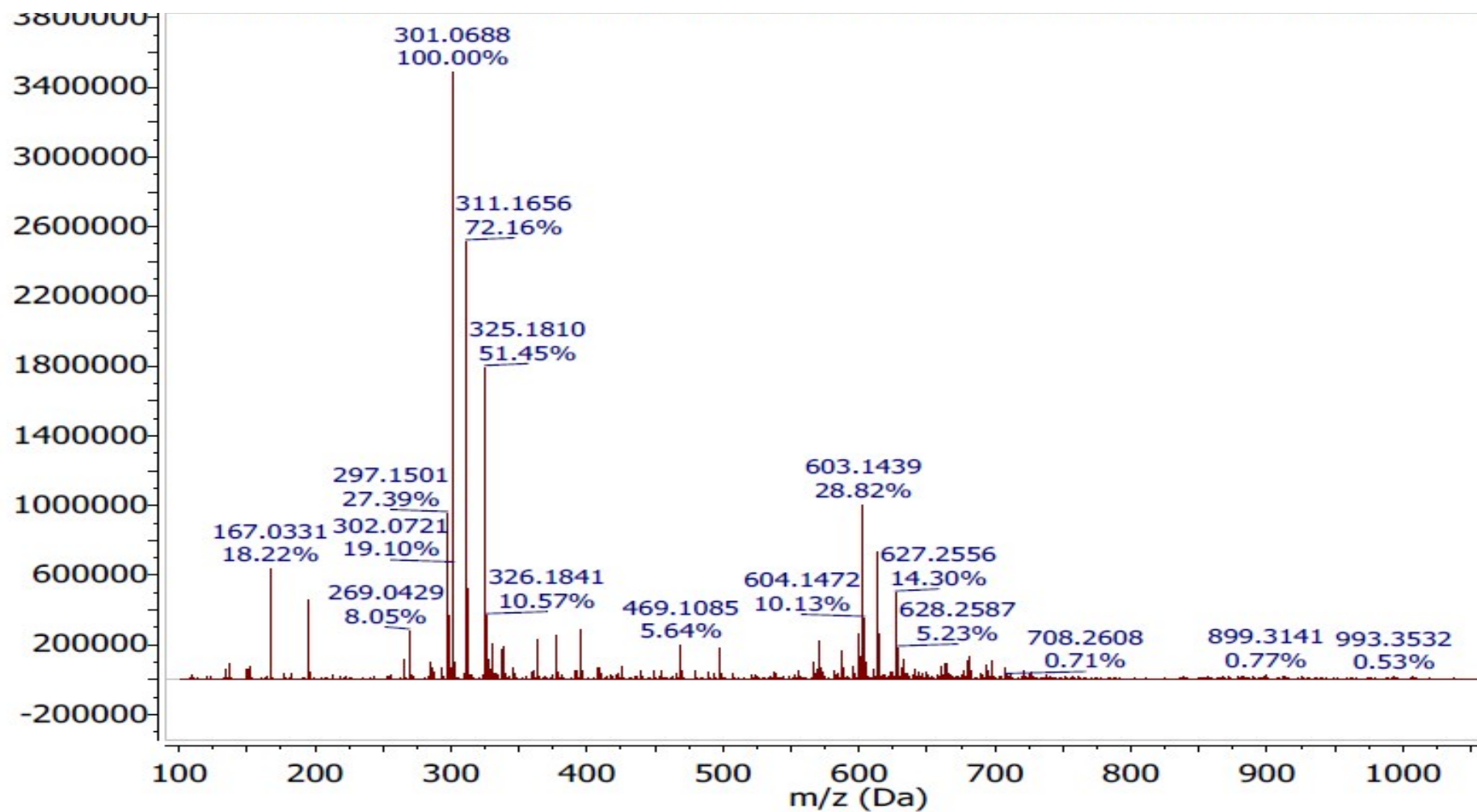


Fig. S22 HRESIMS spectrum of 3,3',4,4'-tetrahydroxy-2-methoxychalcone (7) in negative mode

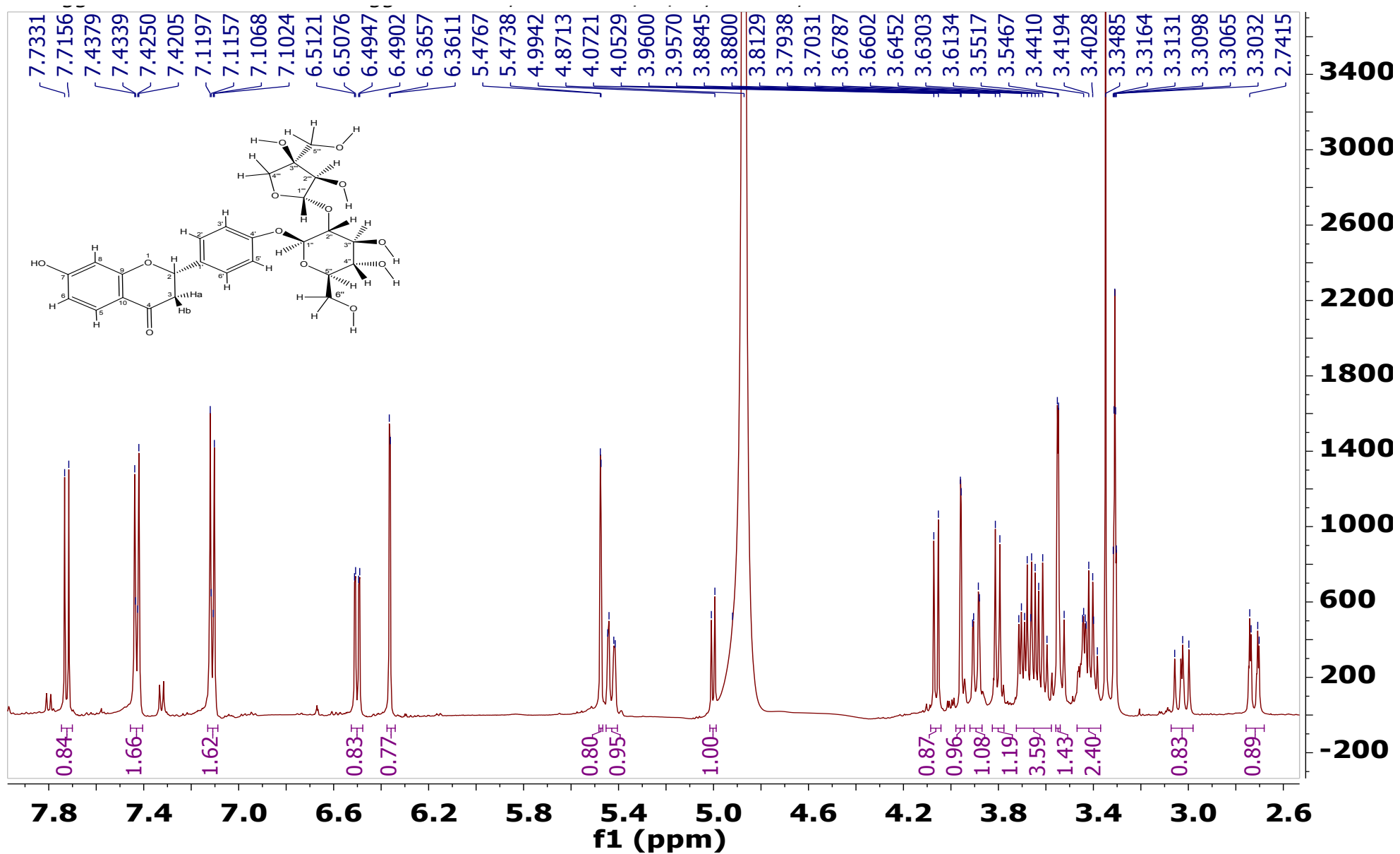


Fig. S23 ¹H-NMR spectrum of liquiritinapioside (8) in CD₃OD at 500 MHz

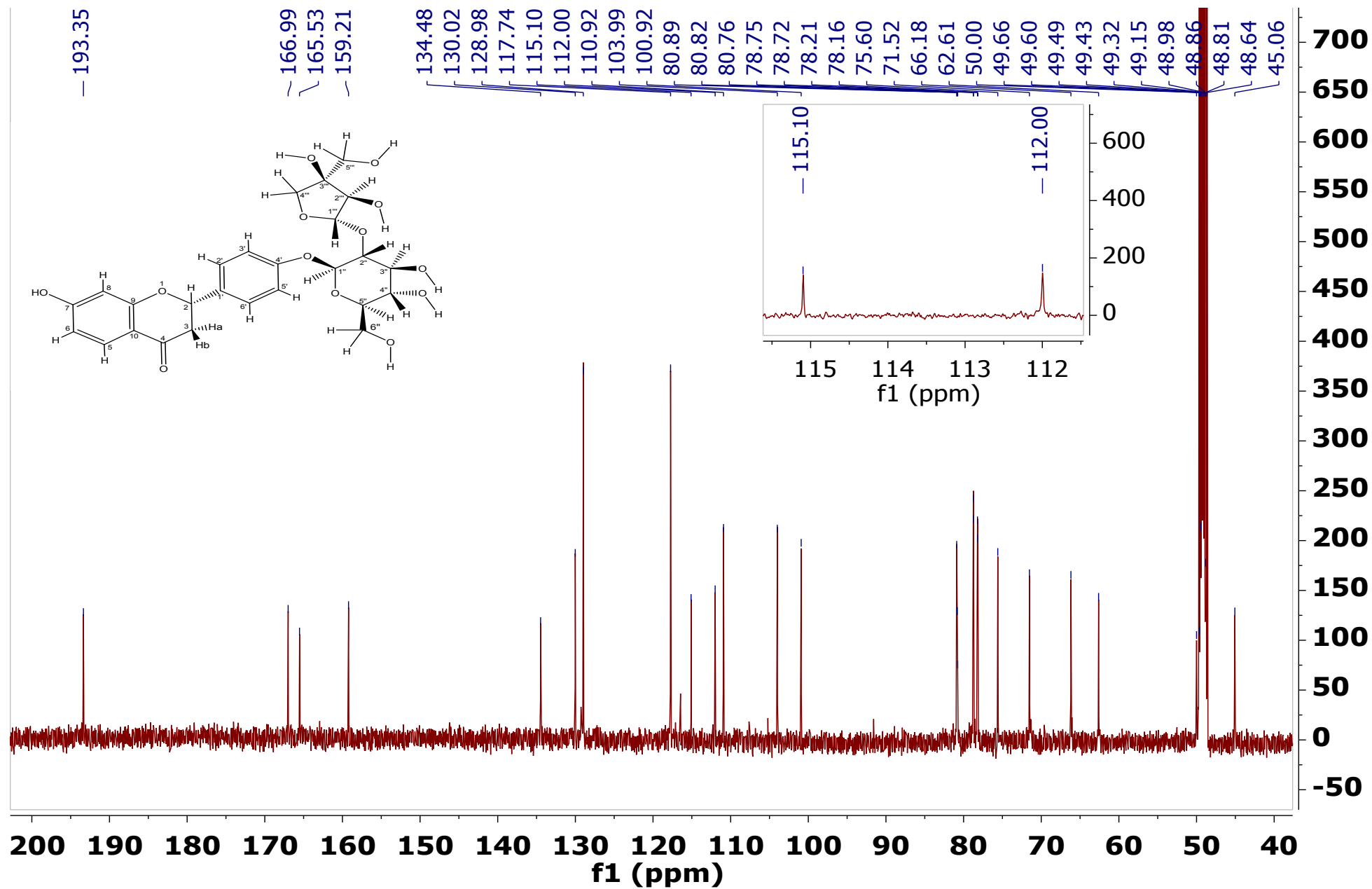


Fig. S24 ¹³C-NMR spectrum of liquiritinapioside (8) in CD₃OD at 125 MHz with expansion at (112-115 ppm)

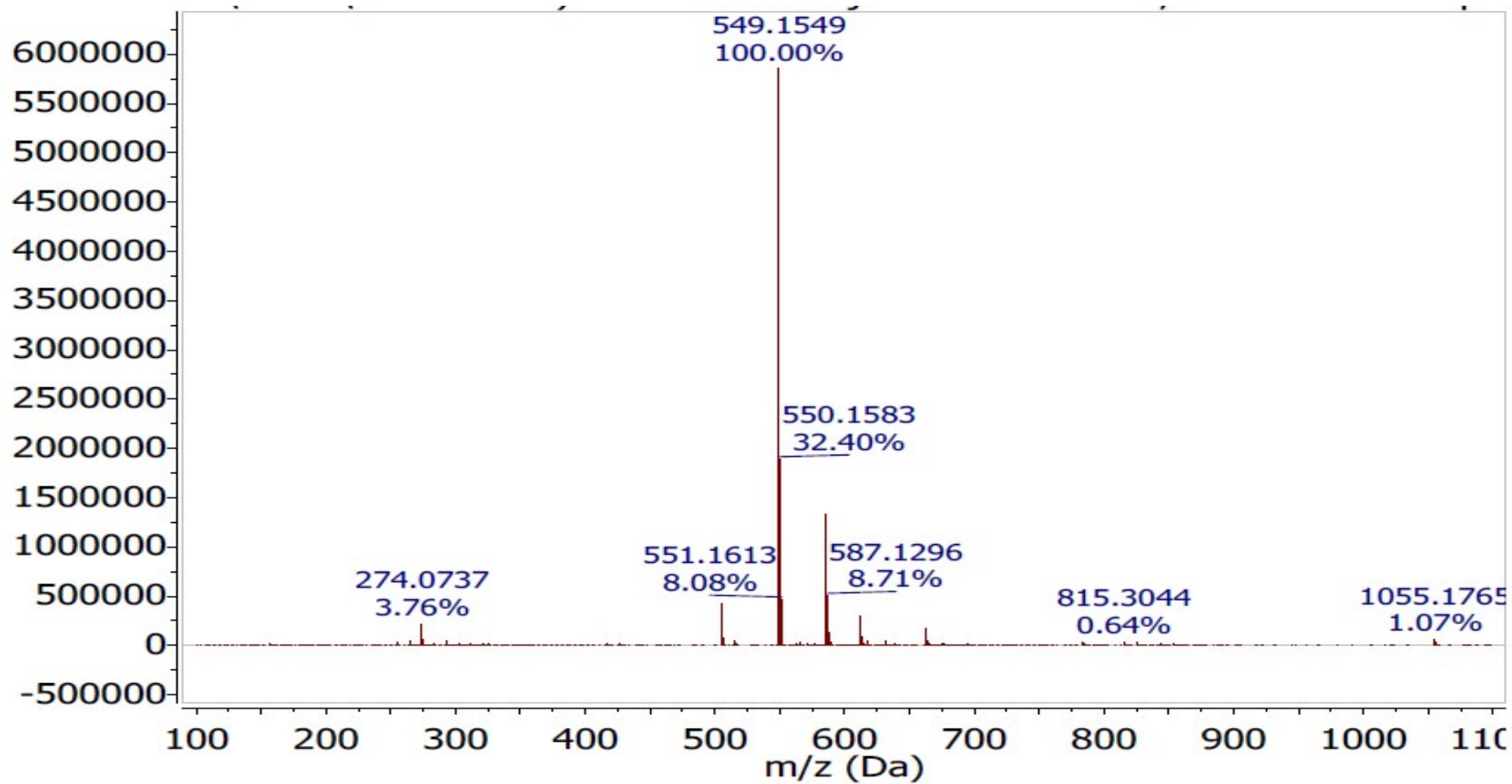


Fig. S25 HRESIMS spectrum of liquiritinapioside (8) in negative mode

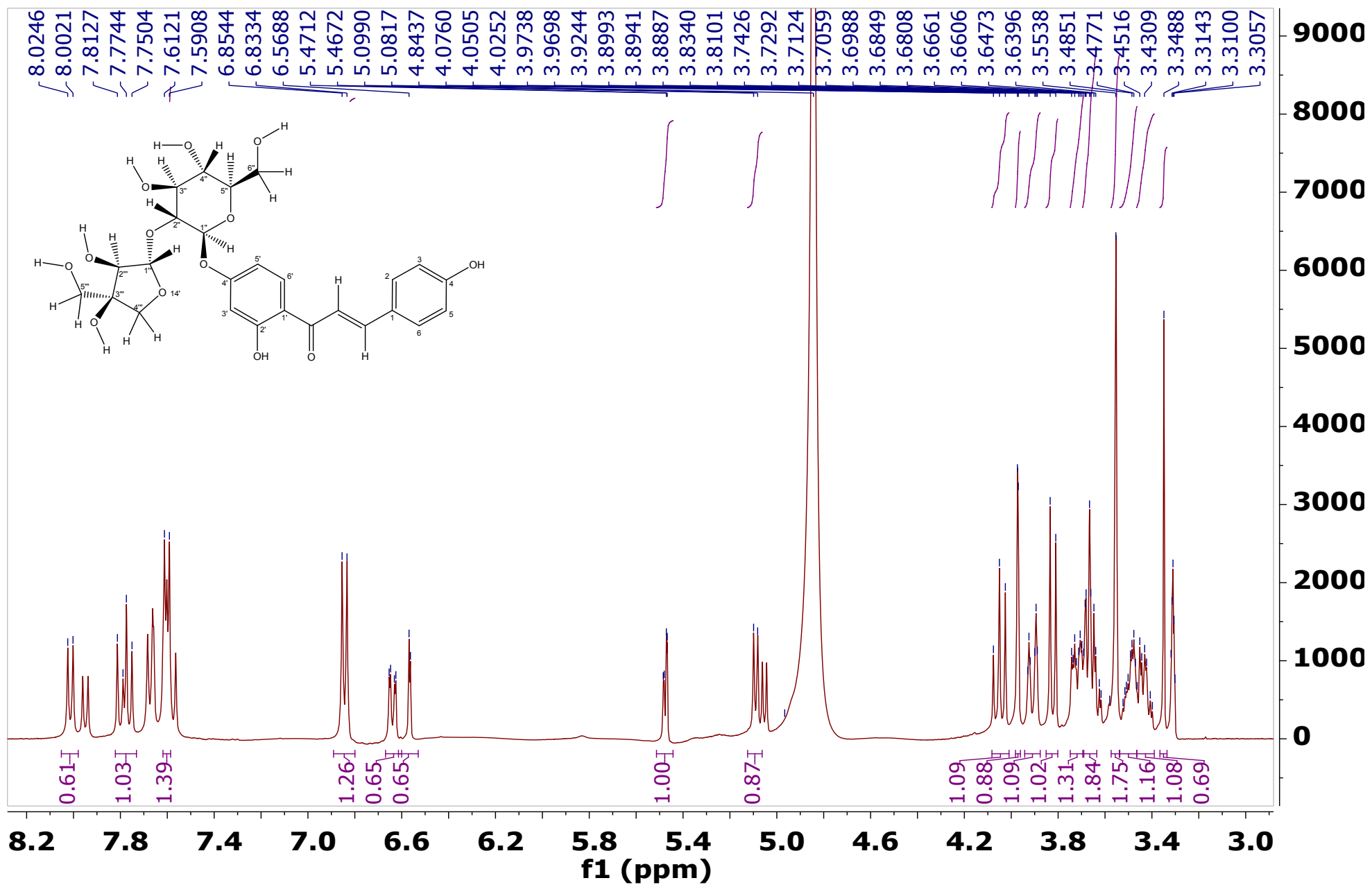


Fig. S26 ¹H-NMR spectrum of isoliquiritigenin-4'-O-β-D-apiosylglucoside (9) in CD₃OD at 400 MHz

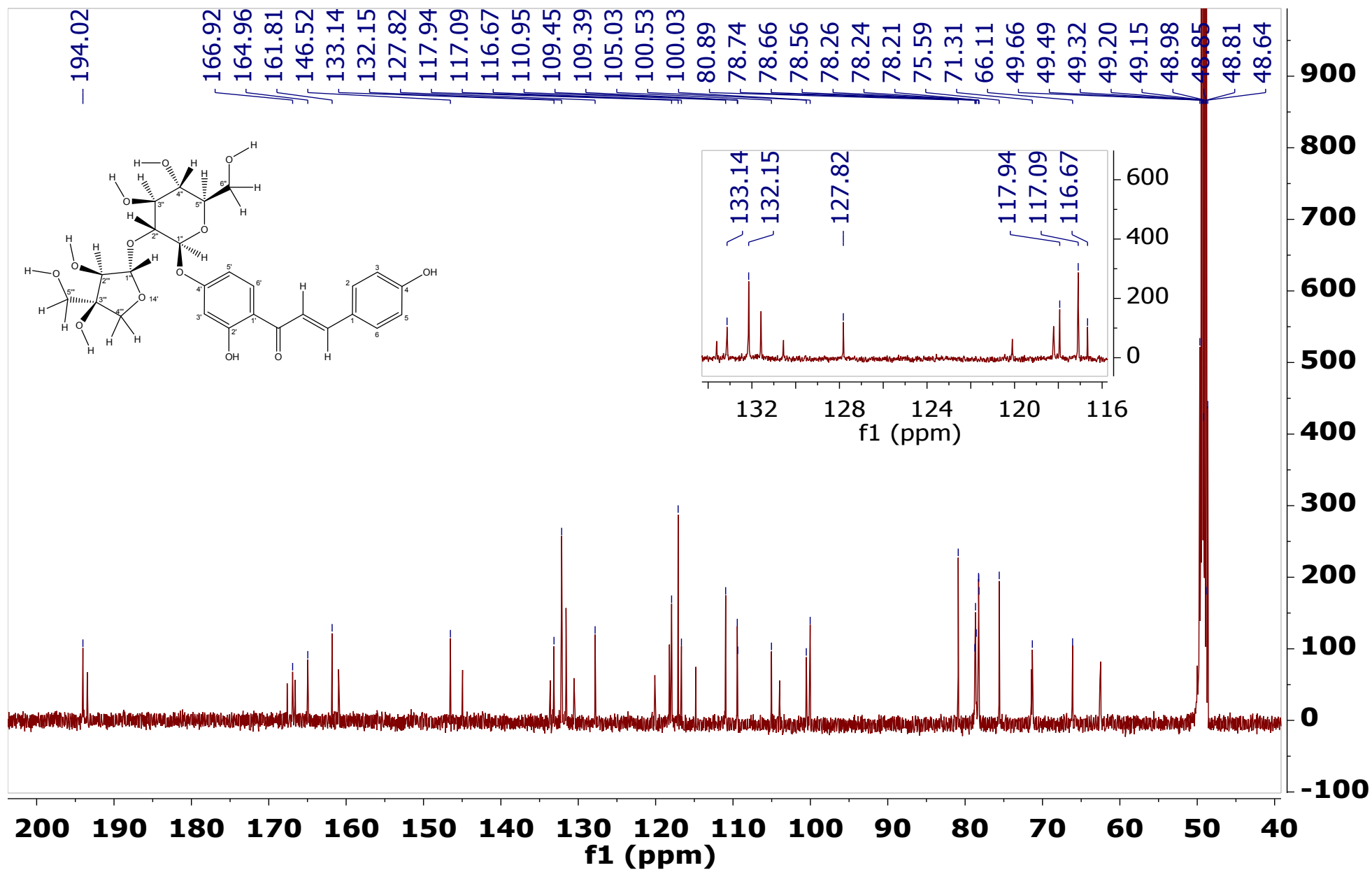


Fig. S27 ^{13}C -NMR spectrum of isoliquiritigenin-4'-O- β -D-aposylglucoside (9) in CD₃OD at 125 MHz with expansion at (115- 130 ppm)

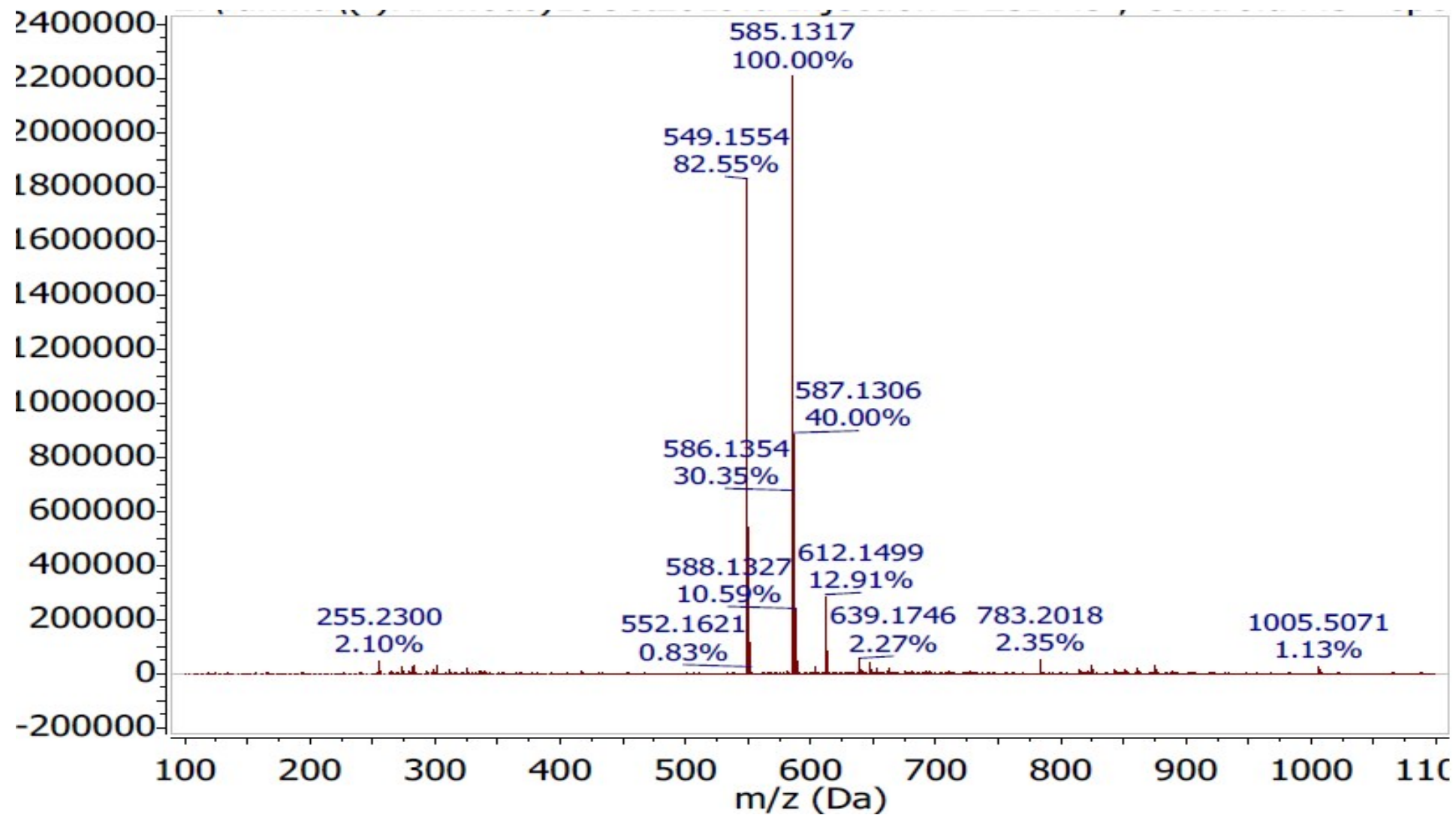


Fig. S28 HRESIMS spectrum of isoliquiritigenin-4'-O-β-D-apiosylglucoside (9) in negative mode

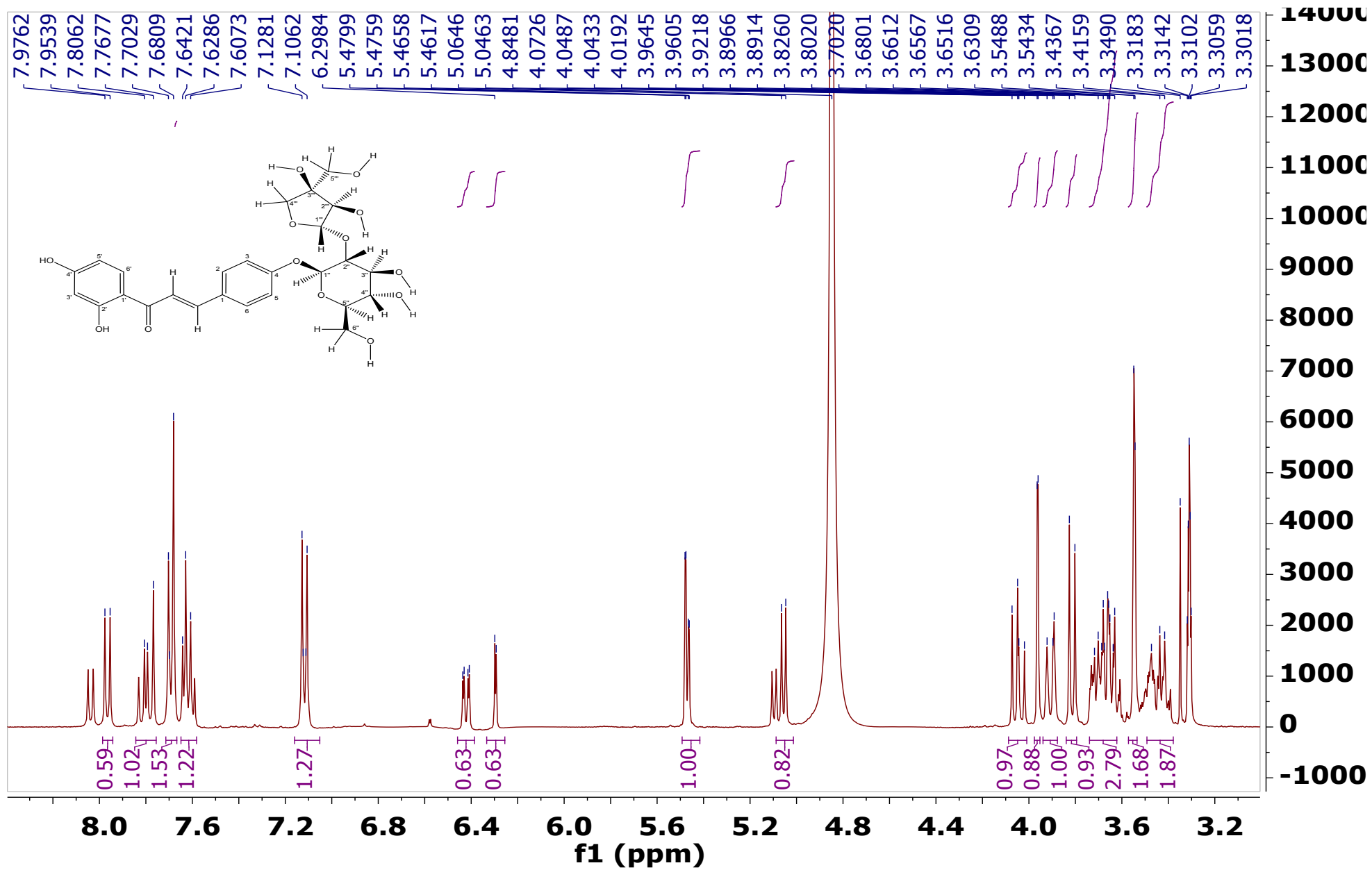


Fig. S29 $^1\text{H-NMR}$ spectrum of isoliquiritigenin-4-O- β -D-aposylglucoside (10) in CD_3OD at 400 MHz

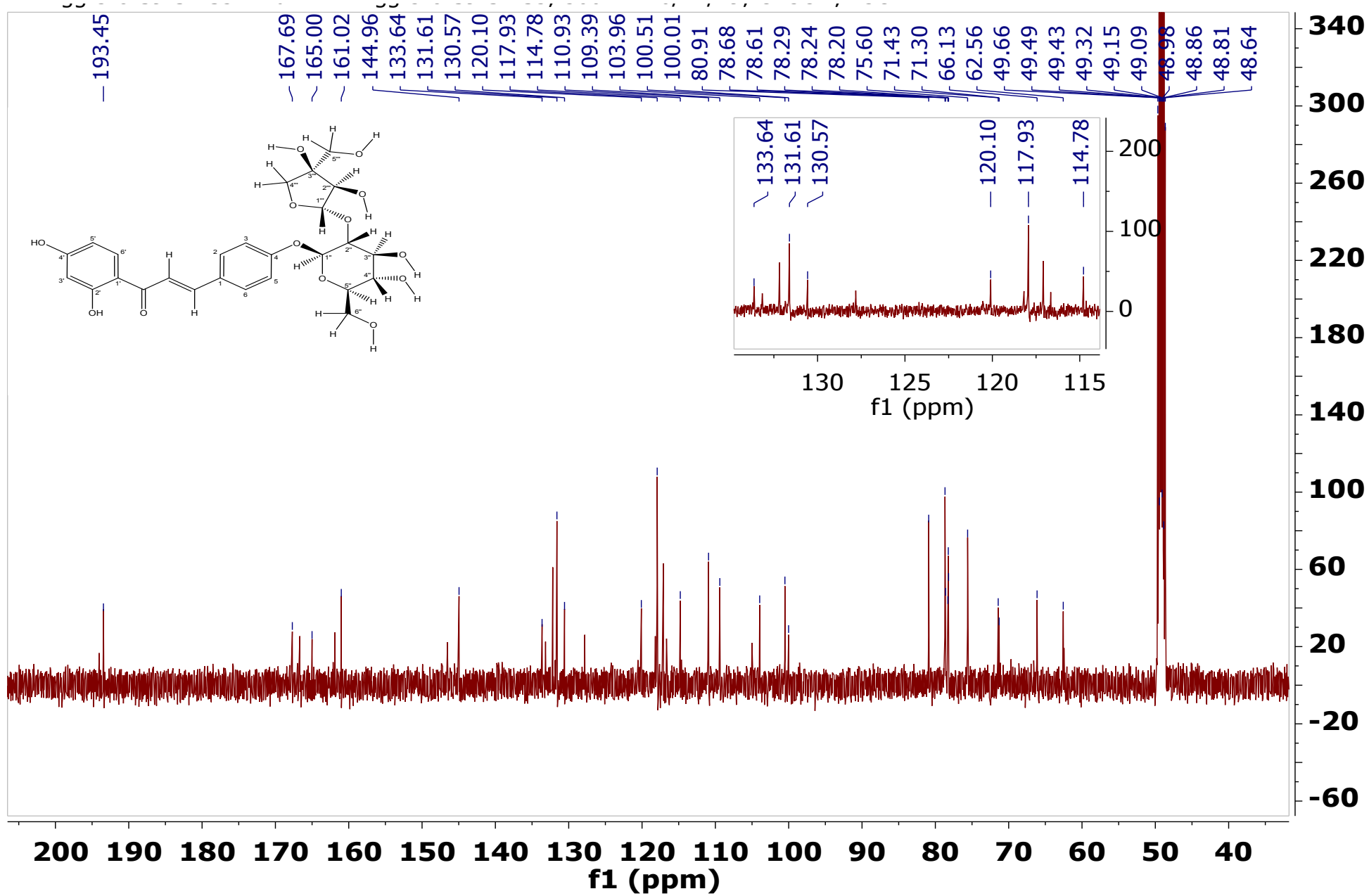


Fig. S30 ^{13}C -NMR spectrum of isoliquiritigenin-4-O- β -D-apiosylglucoside (10) in CD_3OD at 125 MHz with expansion at (115- 130 ppm)

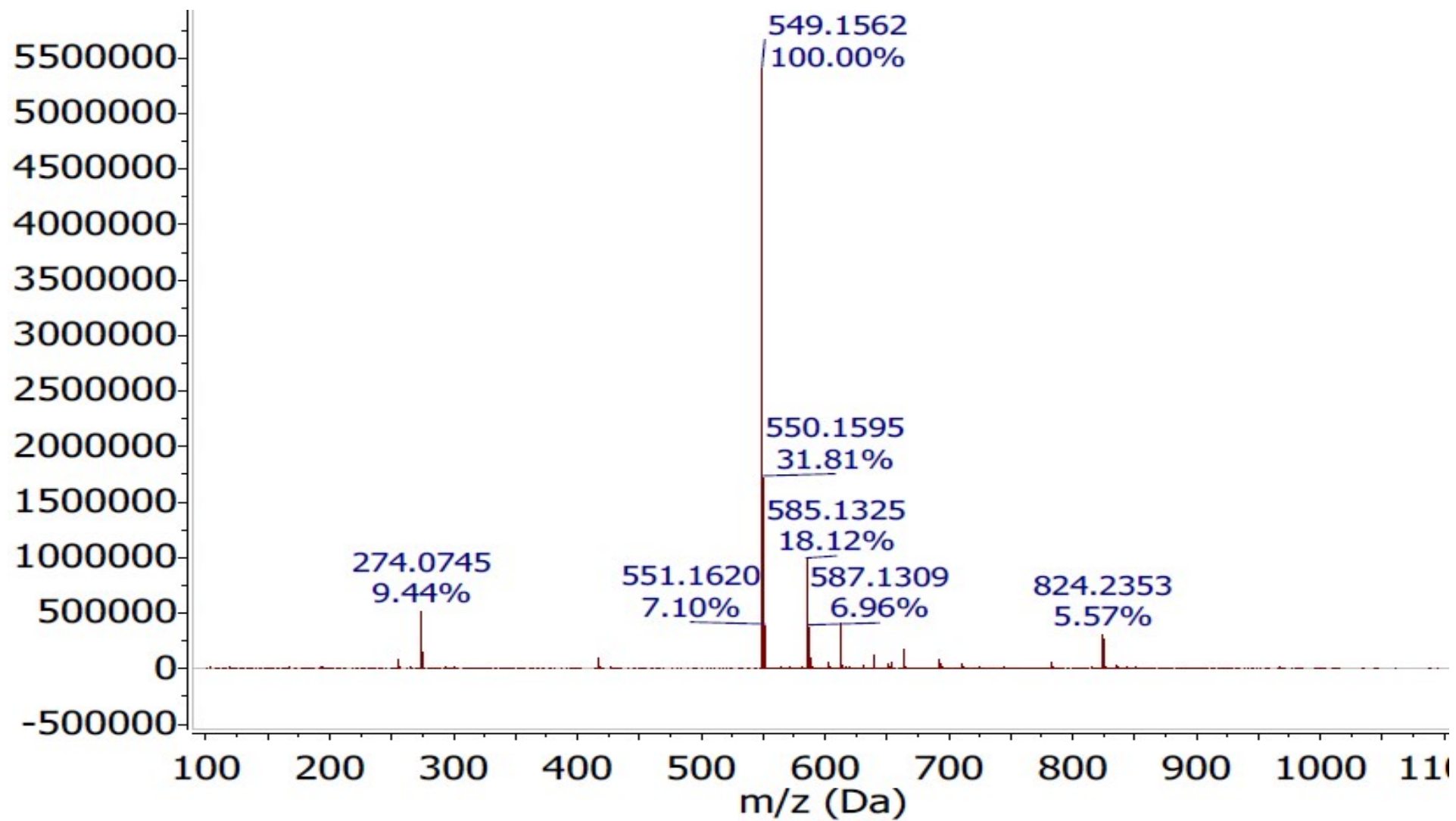


Fig. S31 HRESIMS spectrum of isoliquiritigenin-4-O-β-D-apiosylglucoside (10) in negative mode

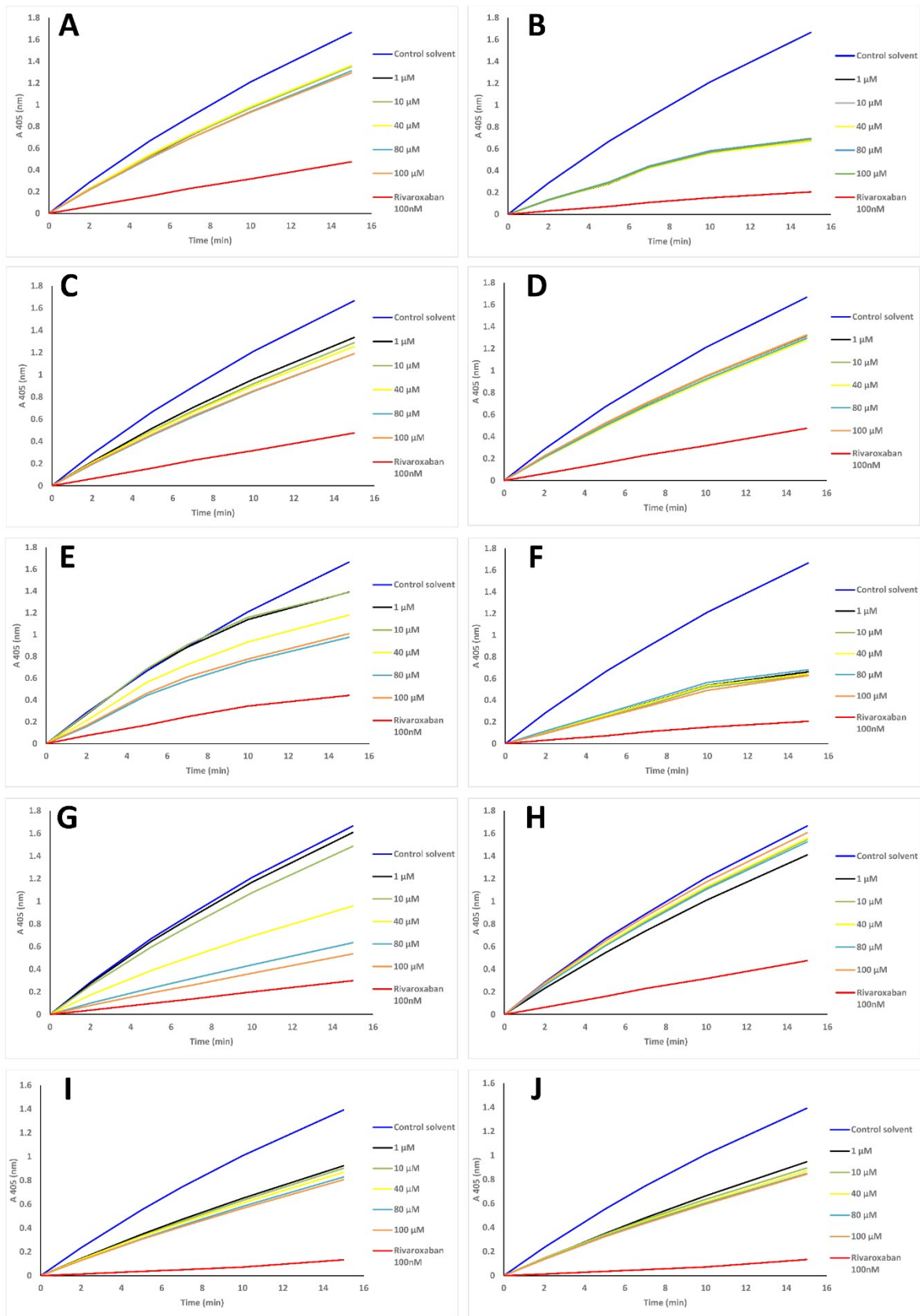


Fig. S32 Absorbance-time curves of FXa mediated hydrolysis of chromogenic substrate using different concentrations of **A.** 7, 4'-dihydroxyflavone, **B.** 7-hydroxy-4'-methoxyisoflavone, **C.** 3-R-glabridin, **D.** isoliquirtigenin, **E.** liquirtin, **F.** naringenin 5-O-glucoside, **G.** 3,3',4,4'-tetrahydroxy-2 methoxychalcone, **H.** liquirtinapioside, **I.** licraside and **J.** isoliquirtinapioside

Table S5. ADMET profile of compounds isolated from licorice compared to synthetic FXa inhibitors

No	Compound	#stars ^a	MW ^b	HBD ^c	HBA ^d	QP logPo/w ^e	QP logS ^f	QPP Caco ^g	CNS ^h	QP logBB ⁱ	QPP MDCK ^j	% Human Oral Absorption ^k	QP Log Khsa ^l	#metab ^m	QP Log HERG ⁿ	Rule Of 5 ^o	Rule Of 3 ^p
A	Rivaroxaban*	0	435.881	1	10.7	2.245	-5.128	425.979	-1	-0.87	837.713	87.151	-0.291	3	-5.884	0	0
B	Apixaban*	0	459.504	2	10.25	2.719	-6.394	171.933	-2	-1.608	73.767	82.875	0.314	4	-6.326	0	1
C	Edoxaban*	0	548.058	1.5	13.5	1.782	-4.603	27.918	-2	-1.347	59.787	37.343	-0.324	6	-5.585	2	0
D	Betrixaban*	0	451.911	2	7.25	4.048	-5.424	503.108	-2	-1.112	512.497	100	0.424	2	-5.84	0	0
1	7, 4'-Dihydroxyflavone	0	254.242	2	4	1.817	-3.271	269.304	-2	-1.031	119.815	81.084	-0.073	2	-5.247	0	0
2	7-hydroxy-4'-methoxyisoflavone	0	268.268	1	4	2.585	-3.422	1274.915	0	-0.448	643.225	100	0.019	2	-5.133	0	0
3	3-R- Glabridin	0	380.483	2	3	5.096	-6.465	1891.682	0	-0.269	985.349	100	1.133	3	-5.129	1	1
4	Isoliquiritigenin	0	256.257	2	3.25	2.074	-3.078	174.841	-2	-1.562	75.117	79.226	-0.084	3	-5.389	0	0
5	Liquiritin	0	418.399	5	12.75	-0.31	-3.232	21.721	-2	-2.737	7.883	49.06	-0.711	7	-5.672	0	2
6	Naringenin 5-O-glucoside	0	434.399	6	13.5	-0.7	-2.996	17.242	-2	-2.898	6.142	32.022	-0.823	8	-5.587	1	2
7	3,3',4,4'-Tetrahydroxy-2-methoxychalcone	0	302.283	4	5.75	0.949	-2.657	58.255	-2	-2.183	22.899	64.096	-0.419	5	-5.105	0	0
8	Liquiritin apioside	6	550.515	7	18.6	-1.293	-2.999	7.111	-2	-3.791	2.358	0	-1.166	9	-6.073	3	2
9	Licraside	7	550.515	7	17.6	-1.054	-2.294	4.771	-2	-4.231	1.532	0	-1.238	8	-6.056	3	2
10	Isoliquirtin apioside	7	550.515	7	17.6	-1.036	-2.318	4.621	-2	-4.246	1.48	0	-1.228	8	-6.043	3	2

***Synthetic FXa inhibitors**

- a) ADME-compliance score – druglikeness parameter (range 0 to 5). b) Molecular Weight of the molecule (range: 130.0 to 725.0)
c) Hydrogen Bond Donor (range: 0.0 to 6.0). d) Hydrogen Bond Acceptor (range: 2.0 to 20.0)
e) Predicted octanol/water partition coefficient (range: -2.0 to 6.5). f) Predicted aqueous solubility (range: -6.5 to 0.5)
g) Predicted Caco cell permeability (range: < 25 is poor and >500 is great). h) Predicted central nervous system activity (-2 (inactive) to +2 (active)).
i) Predicted brain/blood partition coefficient (range: -3.0 to 1.2). j) Predicted apparent MDCK cell permeability (range: < 25 is poor and >500 is great).
k) Percentage of human oral absorption (range: <25 is poor and >80% is high). L) Prediction of binding to human serum albumin (range: -1.5 to 1.5).
m) Number of likely metabolic reactions (range: 1 to 8). n) Predicted IC₅₀ value for blockage of HERG K⁺ channels (concern < -5).
o) Number of violations of Lipinski's rule of five (maximum is 4). p) Number of violations of Jorgensen's rule of three (maximum is 3).